



HAL
open science

Anticipatory smooth eye movements scale with the probability of visual motion: role of target speed and acceleration

Vanessa Carneiro Morita, David Souto, Guillaume S Masson, Anna Montagnini

► To cite this version:

Vanessa Carneiro Morita, David Souto, Guillaume S Masson, Anna Montagnini. Anticipatory smooth eye movements scale with the probability of visual motion: role of target speed and acceleration. 2024. hal-04296695v2

HAL Id: hal-04296695

<https://hal.science/hal-04296695v2>

Preprint submitted on 24 Nov 2024

HAL is a multi-disciplinary open access archive for the deposit and dissemination of scientific research documents, whether they are published or not. The documents may come from teaching and research institutions in France or abroad, or from public or private research centers.

L'archive ouverte pluridisciplinaire **HAL**, est destinée au dépôt et à la diffusion de documents scientifiques de niveau recherche, publiés ou non, émanant des établissements d'enseignement et de recherche français ou étrangers, des laboratoires publics ou privés.

1 **Anticipatory smooth pursuit eye movements scale with the**
2 **probability of visual motion: the role of target speed and**
3 **acceleration**

4 Vanessa Carneiro Morita¹, David Souto², Guillaume S. Masson¹ and Anna
5 Montagnini^{*,1}

6 1 Institut de Neurosciences de la Timone, CNRS & Aix-Marseille Université,
7 Marseille, France

8 2 School of Psychology and Vision Sciences, University of Leicester, Leicester,
9 United Kingdom.

10 * Corresponding author

11

12

13 *Acknowledgements:* This work was funded by the *Agence Nationale de la Recherche*
14 (ANR-PREDICTEYE 18-CE37--0019 to GSM, AM) and the *Fondation pour la Recherche*
15 *Médicale* (Equipe FRM 2018 to GSM) and by Aix-Marseille Université (PhD Doctoral
16 extension funding to VCM). We would like to thank Mr Alexis Ulian for helping in
17 the data collection of the Experiment 2A as part of his Master internship.

18 Abstract

19 Sensory-motor systems can extract statistical regularities in dynamic uncertain
20 environments, enabling quicker responses and anticipatory behavior for expected
21 events. Anticipatory smooth pursuit eye movements (aSP) have been observed in
22 primates when the temporal and kinematic properties of a forthcoming visual
23 moving target are fully or partially predictable. To investigate the nature of the
24 internal model of target kinematics underlying aSP, we tested the effect of varying
25 the target kinematics and its predictability. Participants tracked a small visual target
26 in a constant direction with either constant, accelerating or decelerating speed.
27 Across experimental blocks, we manipulated the probability of each kinematic
28 condition varying either speed or acceleration across trials; with either one
29 kinematic condition (providing certainty) or with a mixture of conditions with a
30 fixed probability within a block. We show that aSP is robustly modulated by target
31 kinematics. With constant-velocity targets, aSP velocity scales linearly with target
32 velocity in blocked sessions, and matches the probability-weighted average in the
33 mixture sessions. Predictable target acceleration does also have an influence on aSP,
34 suggesting that the internal model of motion which drives anticipation contains
35 some information about the changing target kinematics, beyond the initial target
36 speed. However, there is a large variability across participants in the precision and
37 consistency with which this information is taken into account in order to control
38 anticipatory behavior.

39 Introduction

40 Smooth pursuit eye movements allow us to maintain the image of a moving
41 object of interest steady on the retinas. To do so, tracking eye movements rely
42 primarily on the neural representation of the moving target's speed and direction
43 (Carl & Gellman, 1987; Lisberger & Westbrook,; Tychsen & Lisberger, 1986). When
44 the target moves at constant speed across the visual field, the eyes start accelerating
45 in the same direction as the target motion with a short latency (~100-130 ms in
46 humans; Carl & Gellman, 1987). In the optimal speed range for human pursuit (i.e.
47 below 20-30°/s), the eyes typically reach a steady state velocity close to the target's
48 velocity within ~300 ms from visual motion onset. Steady-state smooth tracking, in
49 close coordination with the so-called catch-up saccades can dynamically maintain a
50 good alignment between the fovea and the target retinal image position (Carl &
51 Gellman, 1987; Orban De Xivry & Lefèvre, 2007). Even though natural objects
52 rarely move at a constant velocity, only a few studies have investigated eye tracking
53 behavior for accelerating (or decelerating) targets. Those studies reported that
54 humans are indeed able to track visible targets with smoothly-varying speed (e.g.
55 Bennett & Benguigui, 2013; Kreyenmeier et al., 2022), but with weak accuracy. Like
56 perceptual discrimination judgments, tracking eye movements discriminate poorly
57 between target accelerations as compared to target speeds in humans (e.g.,
58 Watamaniuk & Heinen, 2003; Kowler & McKee, 1987) and macaque monkeys
59 (Lisberger & Movshon, 1999).

60 Most of the early work on pursuit eye movements and visual
61 speed/acceleration processing were concerned with the online control. However,
62 our dynamic environment is often, at least in part, predictable, because either the
63 motion is produced by our own body (e.g., Gauthier et al., 1988; Landelle et al.,
64 2016), or it can be inferred from general prior knowledge, past experience or
65 perceptual cues about an object's motion (Kowler et al., 2019). For instance, when a
66 target's velocity changes in a periodic way (e.g., sinusoidal motion), ocular tracking
67 can rapidly take advantage of this predictable motion such that, after only a few
68 cycles, the fovea is aligned to the target position with nearly no lag (Kowler &
69 Steinman, 1979a). Moreover, motion predictability allows anticipation of the target
70 motion onset, or target reappearance after a transient occlusion (e.g. Dodge et al.,
71 1930; for a review, see Kowler et al., 2019 and Fukushima et al., 2013). These
72 anticipatory smooth pursuit eye movements (aSP) are thought to help in quickly
73 reducing the retinal position and velocity errors during the early phase of
74 visually-guided pursuit (e.g. Kao & Morrow, 1994).

75 Large efforts have been devoted to understanding what kind of signals drive
76 anticipatory responses (Kowler et al., 2019). The underlying computational
77 mechanisms of aSP are however still not fully understood. Empirically, target
78 motion predictability can be manipulated across different time scales (e.g. across or
79 within trials in a standard visuomotor experiment) and repetition schedules. Our
80 group, and others have previously shown that aSP amplitude is proportional to the
81 probability of a given target motion direction in a direction-biased task (Damasse et
82 al., 2018; Montagnini et al., 2010; Rubinstein et al., 2024; Santos & Kowler, 2017;

83 Wu et al., 2021). Expectation for a given target speed also modulates aSP:
84 anticipatory eye velocity increases with speed predictability, in a random versus
85 fully predictable speed design (e.g., Heinen et al., 2005; Jarrett & Barnes, 2002; Kao
86 & Morrow, 1994). aSP also depends on the recent trial history of target speed (Maus
87 et al. 2015). However, it has not been tested whether aSP exhibits the same linear
88 dependency upon speed probability as it does for direction probability.

89 Predictive aSP has been extensively investigated for simple target trajectories
90 of constant speed and/or direction (e.g., among many others, in Barnes & Asselman,
91 1991; Heinen et al., 2005; Kowler & Steinman, 1979b). However, much less is
92 known about aSP for accelerating targets and the contribution of acceleration
93 signals to the internal representation of motion raises several questions. First, it is
94 still not known if acceleration is taken into account when preparing for anticipatory
95 movements, or if the latter are based on simple estimates approximating the target
96 motion profile (e.g. instantaneous at some critical moments, or time-averaged speed,
97 Bennett, Orban De Xivry, et al., 2010). Second, most of the previous studies have
98 investigated acceleration-based predictive behavior only on a short time scale,
99 namely during the transient occlusion of a moving target with an accelerating
100 profile (Bennett et al., 2007, 2010; Bennett & Barnes, 2006).

101 From these previous studies, target acceleration does not appear to be fully
102 integrated in predictive pursuit. For instance, when an accelerating target is
103 occluded after a short presentation of accelerating motion (~ 200 ms), eye velocity
104 during the blanking period reduces, and its predictive reacceleration prior to the

105 target reappearance is not influenced by the target acceleration (Bennett et al.,
106 2007). However, if the target visibility window before the occlusion is long enough
107 (> 500 ms), eye velocity reduces during the blanking period, but recovers in an
108 acceleration-scaled manner prior to the target reappearance (Bennett, Orban De
109 Xivry, et al., 2010). Moreover, target acceleration is not appropriately taken into
110 account neither in a task where participants are asked to track a target and, after a
111 period of occlusion, to predict the target position, or to predict when the target is
112 going to reach a certain position (Bennett & Benguigui, 2013; Kreyenmeier et al.,
113 2022). However, one of the very few studies addressing the effect of acceleration
114 predictability on a longer time scale (blocked design) showed that the amplitude of
115 aSP observed before the target reappearance in an occlusion paradigm scales with
116 target acceleration (Bennett & Barnes, 2006). Here, we aimed at better
117 understanding how target motion acceleration shapes aSP when the predictability of
118 the kinematic profile is manipulated on a relatively long timescale, namely across
119 blocks of several tenths of trials.

120 In the present study we tested the following hypotheses: 1) Anticipatory
121 smooth pursuit eye velocity scales linearly with target speed probability (similar to
122 direction probability, Damasse et al. 2018, Santos et al. 2017), across experimental
123 blocks with fixed probability; 2) Anticipatory eye velocity is modulated by target
124 acceleration and 3) it scales with the probability of the accelerating motion. To test
125 these hypotheses, we analyzed anticipatory oculomotor behavior for targets moving
126 in a fully predictable direction but with different speeds and accelerations. We
127 manipulated the probability of each kinematic condition across blocks. We showed

128 that target speed probability influences aSP similarly to motion direction
129 probability, with a linear dependence of aSP velocity upon target speed probability.
130 We also showed that aSP can be driven by predictable accelerating targets, in a way
131 that accounts for the expected change in target velocity and for its probability, even
132 though with large inter-individual variability.

133 **Methods**

134 **Participants**

135 Twenty-nine healthy adult volunteers signed an informed consent to
136 participate in the experiments presented in this study. The experimental protocol
137 was approved by the Ethics Committee *Comité de Protection des Personnes OUEST III*
138 (CPP reference: PredictEye-2018-A02608-47), in full respect of the Helsinki
139 declaration guidelines. Three of the authors (AM, GM, DS) participated in
140 Experiment 1A (n=3), two of the authors (AM, VCM) participated in Experiment
141 1B-2A (n=13) and one of the authors (VCM) participated in Experiment 2B (n=5)
142 and in Experiment 3 (n=8). In Experiment 1A, anticipatory eye movements and
143 initial pursuit were recorded with high precision by using the scleral search coil
144 technique (Robinson, 1963) in a small participant sample. A preliminary version of
145 the results from Experiment 1A was presented previously at the VSS conference
146 (Souto et al., 2008). The core finding of this experiment motivated Experiments
147 1B-2A-2B, that were run with a larger sample of participants, a smaller subset of
148 probability conditions, and using a less invasive technique (video eye tracking).
149 Experiment 3 was designed to test the effect of acceleration on anticipatory eye

150 speed in fully predictable blocks, again using a non-invasive eye recording
151 technique.

152 **Stimuli and procedure**

153 In all experiments, participants were instructed to visually track a small
154 moving target by smoothly pursuing it with their eyes, as accurately as they could,
155 while their eye movements were recorded. We used different materials across
156 experiments.

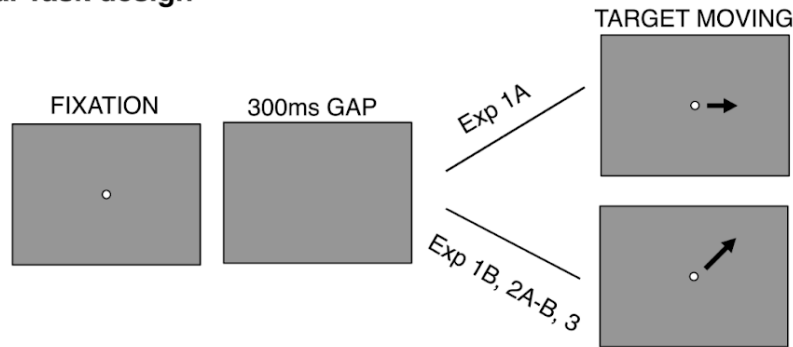
157 **Experiment 1A**

158 The detailed methods are described elsewhere (Wallace et al. 2005). Briefly,
159 a PC running the REX package controlled both stimulus presentation and data
160 acquisition. Stimuli were generated with an SGI Fuel workstation (ABC Corp., New
161 York, USA, no longer available) and back-projected onto a large translucent screen
162 (80° x 60°, viewing distance: 1m) using a Barco 908s video-projector (1280", 1024
163 pixels at 76 Hz). Oculomotor recordings were collected using the scleral search coil
164 technique (Collewijn et al. 1975).

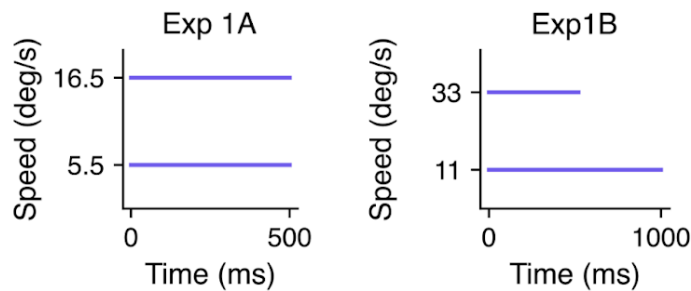
165 This experiment probed aSP in different target speed probability contexts
166 (**Figure 1a**). Each trial started with a white fixation point, located at the center of
167 the screen for a random duration between 300 and 450 ms, on a black uniform
168 background (luminance $< 1 \text{ cd/m}^2$). If the participant fixated accurately (i.e. within
169 a 2°-side, square electronic window) during the last 200 ms, the fixation target was
170 extinguished and followed by a fixed-duration, 300-ms empty screen. At the end of

171 this gap, the target (a white, gaussian-windowed circle, 0.2° std, maximum
172 luminance 45 cd/m^2) appeared at the center of the screen and started moving
173 horizontally to the right, for a fixed period of 500 ms. The target speed was either
174 $5.5^\circ/\text{s}$ (low speed, LS) or $16.5^\circ/\text{s}$ (high speed, HS). In each experimental block, a
175 different target speed-probability condition defined the proportion of trials at high
176 speed ($P(\text{HS}) = 0, 0.1, 0.25, 0.5, 0.75, 0.9$ and 1). The complementary proportion of
177 trials had a low-speed target motion ($P(\text{LS}) = 1 - P(\text{HS})$). Participants completed 500
178 trials per block, except for the $P(\text{HS}) = 0$ and $P(\text{HS}) = 1$ conditions where only 250
179 trials were completed. One or two blocks were completed in a day, with the
180 constraint of not exceeding a total of one hour of duration.

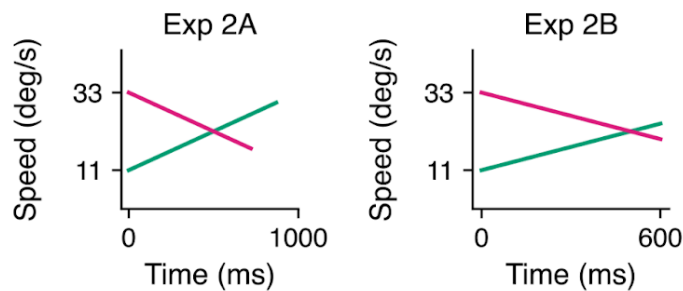
a. Task design



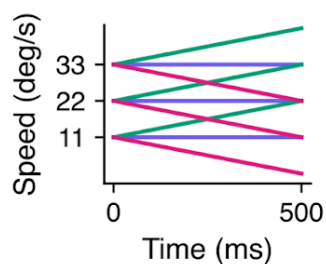
b. Experiment 1



c. Experiment 2



d. Experiment 3



e. ANEMO fit

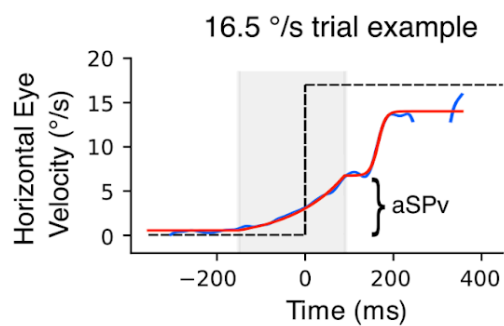


Figure 1. Experimental designs. (a). Each trial started with a fixation point displayed at the center of the screen for a random period, followed by a gap of 300 ms. The target then appeared at the center of the screen and started moving. (b). **Experiment 1.** In Experiment 1A, the target moved horizontally to the right at one of the two constant speeds (5.5 or 16.5 °/s, in blue). The probability of a high-speed ($P(HS)$, $v=16.5$ °/s) vs a low-speed

($P(\text{LS}) = 1 - P(\text{HS})$, $v = 5.5^\circ/\text{s}$) trial was varied between experimental blocks with 7 different values of $P(\text{HS})$ (0, 0.1, 0.25, 0.5, 0.75, 0.9, 1). In Experiment 1B the target always moved in a fixed direction, chosen between one of the four diagonals (counterbalanced between participants). We displayed two different constant target speeds (v_{11c} and v_{33c} , of 11 and 33 $^\circ/\text{s}$, respectively, in blue). Conditions were designed with a constant target displacement, and we manipulated the probability of the target kinematics in each experimental block with the probability of v_{11c} spanning the values (0, 0.3, 0.7, 1) and $P(v_{33c}) = 1 - P(v_{11c})$. **(c) Experiment 2.** Experiment 2A followed a design similar to Exp 1B, but this time the target kinematics included acceleration conditions. The initial speed was kept the same as in Exp 1B, but the target with initial speed at 11 $^\circ/\text{s}$ accelerated (v_{11a} , $a = 22^\circ/\text{s}^2$, in green) and the target with initial speed at 33 $^\circ/\text{s}$ decelerated (v_{33d} , $a = -22^\circ/\text{s}^2$, in pink). In Experiment 2B, target kinematics were the same as in Exp 2A, except the time duration of the target motion was kept constant at 600 ms. **(d) Experiment 3.** We displayed three different initial speeds (v_{11} , v_{22} , v_{33} of 11, 22 and 33 $^\circ/\text{s}$, respectively) combined with three different acceleration values (a , c and d , of 22, 0 and $-22^\circ/\text{s}^2$, in green, blue and pink respectively) in fully predictable blocks. Target motion duration was kept constant and lasted 500ms. **(e) Model fitting of eye velocity profiles in individual trials.** The bottom panel shows an example of the eye velocity trace (blue curve) and of the ANEMO model fit (red curve, Pasturel et al., 2018) in an individual trial. The selected model fitted an exponential function to the anticipatory phase, and a sigmoid to the initial visually-guided pursuit phase. From this model we extracted the maximum of the anticipatory velocity (aSPv). The model fitting procedure for Experiments 1B, 2A, 2B and 3 was similar to Experiment 1A.

181 Experiments 1B, 2 and 3

182 Experiment 1B-2A

183 The same group of participants took part in Experiments 1B and 2A. Stimuli
184 were presented using the Psychtoolbox (Brainard, 1997) package for MATLAB. A
185 Display++ monitor (CRS Ltd., Rochester, UK) with a refresh rate of 120 Hz was
186 placed at 57 cm distance in front of the participant. Eye movements were recorded
187 using an Eyelink1000, an infrared video-based eye tracker (SR Research Ltd.,
188 Ottawa, Canada). This experiment probed aSP with different target constant and
189 varying speed conditions, while manipulating the probability of each condition.

190 With respect to Experiment 1A, a larger pool of participants was tested with a
191 different set of target speed values and a smaller set of speed probabilities and fewer
192 trials per condition. Because several studies have reported anisotropies for saccadic
193 and smooth pursuit eye movements across different directions (e.g., Grasse &
194 Lisberger, 1992; Ke et al., 2013; Rottach et al., 1996; Takeichi et al., 2003), we
195 decided to investigate whether the results observed in Experiment 1A can be
196 generalized across target motion directions. Accordingly, in Experiment 1B-2A the
197 target moved along one of the four diagonal directions, counterbalanced between
198 participants.

199 **Figure 1a** shows the experimental design. Each trial started with a white
200 fixation dot in the center of the screen for a random interval between 300 ms and
201 600 ms. This fixation period was followed by a 300 ms gap. At the end of this
202 period, the target (a white circle of 0.6° diameter, maximum luminance 45 cd/m^2 on
203 a black background with luminance $< 1 \text{ cd/m}^2$) appeared at the center of the screen
204 and started moving in one of the four diagonal directions (always the same for one
205 participant) with different target kinematics conditions: the target speed was either
206 constant (v11c and v33c; 11 and $33^\circ/\text{s}$ respectively), uniformly accelerating (v11a;
207 starting from $11^\circ/\text{s}$, $a = 22^\circ/\text{s}^2$), or decelerating (v33d; starting from $33^\circ/\text{s}$, $a = -22$
208 $^\circ/\text{s}^2$). In Experiments 1B and 2A, target motion duration was adapted to the target
209 kinematic properties in order to achieve a similar spatial displacement on the screen
210 across conditions: in practice target movement lasted 1 and 0.52 s for v11c, and
211 v33c, respectively, 0.87 s for v11a, and 0.72 s for v33d.

212 Participants first completed 4 blocks of 100 trials with a single target
213 kinematics condition (v11c, v33c, v11a, v33d, presented in randomized order across
214 participants). Notice that these conditions can be considered as a probability of 1 for
215 each kinematic value. Next, the probability of the different target kinematics was
216 manipulated across blocks of 200 trials each. For blocks with constant speed, we
217 used v11c and v33c, with $P(v33c)$ being equal to either 0.3 or 0.7 and
218 $P(v11c)=1-P(v33c)$. The two probability levels were presented in random order
219 across participants. For blocks with accelerating speed, $P(v33d)$ could be either 0.3
220 or 0.7 ($P(v11a)=1-P(v33d)$). Again, these two probability conditions were
221 randomly interleaved.

222 *Experiment 2B*

223 Having different motion durations across conditions might have introduced
224 some confounds affecting anticipatory behavior. First, estimates of target
225 acceleration can be impaired if the target motion is presented too briefly (Bennett,
226 De Xivry, et al., 2010; Bennett et al., 2007). Second, if anticipatory behavior relies
227 on the estimate of mean target velocity, rather than on its accelerating dynamics
228 (Brouwer et al., 2002; Gottsdanker et al., 1961; Schmerler, 1976), then the duration
229 of the visual motion epoch might influence the mean velocity estimate for targets
230 with accelerating speed. Therefore, we ran an additional control experiment (Exp
231 2B) with the same design as Exp 2A but with one main difference: target motion
232 duration was held constant (600ms), resulting in different target final positions
233 across conditions.

234 **Experiment 3**

235 While Experiments 1 and 2 were designed to probe the effects of probability
236 manipulation for both constant and accelerating target motion, we did not directly
237 address whether and how the accelerating motion of predictable accelerating targets
238 drive anticipatory eye movements. Most of the literature on smooth pursuit focus on
239 constant speed targets, and the very few studies manipulating acceleration focuses
240 on the effects of this manipulation on the visually-guided pursuit (Brostek et al.,
241 2017; Krauzlis & Lisberger, 1994) or short-term predictive tracking (e.g. blanking
242 paradigm, Bennett et al., 2007, 2010; Bennett & Barnes, 2006; Bennett & Benguigui,
243 2013). Interestingly, Bennett & Barnes (2006) showed that for a fixed initial target
244 speed and when accelerating target motion is presented in a blocked design,
245 anticipatory eye movements scale with target acceleration. In order to better
246 understand the relationship between target acceleration and anticipatory eye
247 movements, we ran Experiment 3 (**Figure 1d**), with a *fully-crossed* design, in which
248 the target could take one out of three possible initial speeds (v_{11} , v_{22} , and v_{33} of
249 11, 22, and 33 °/s, respectively) and one out of three possible acceleration values
250 (of 22, 0 and -22 °/s², labeled as “a” for *accelerating*, “c” for *constant* and “d” for
251 *decelerating*, respectively). This design yielded in nine blocks of fully-predictable
252 target motion. In all blocks, the target motion duration was held constant to 500 ms.
253 Participants completed 100 trials in each block with v_{11} and v_{22} as initial speeds,
254 and 120 trials in each block with v_{33} as initial speed. The small difference in the
255 number of trials was introduced to compensate for the higher number of excluded
256 trials for the data analysis, due to a higher occurrence of saccades around target

257 motion onset, a phenomenon already observed in the previous experiments when
258 the fastest speed (v33) was presented.

259 **Eye-movements recording and preprocessing**

260 For Experiment 1A, the analog voltage measure collected with the scleral coil
261 technique and reflecting the right-eye rotation was low-pass filtered (DC-130 Hz)
262 and digitized with 16-bit resolution at 1000 samples per second (to obtain the eye's
263 horizontal and vertical position). For Experiments 1B, 2A, 2B and 3, the right-eye
264 horizontal and vertical position was recorded with an infrared video-based eye
265 tracker, EyeLink 1000 (SR Research), at 1 kHz.

266 For all sets of recorded eye movements, position data was converted in an
267 ASCII format. After conversion, the ANEMO toolbox (Pasturel et al., 2018) and
268 custom-made python scripts were used to pre-process the data. Position data was
269 low-pass filtered (acausal second-order Butterworth low-pass filters, 30 Hz cut-off),
270 numerically differentiated to get the eye velocity in degrees per second and then
271 de-saccaded using ANEMO's implementations. In practice, saccade detection was
272 implemented by jointly applying the absolute eye velocity threshold criterion
273 (30°/s, by default in the Eyelink system) and the relative velocity threshold (akin to
274 the method proposed by Engbert & Kliegl, 2003). The epochs corresponding to
275 detected saccades were removed from analysis (given not-a-number values). Trials
276 with more than 40% of missing data points in the [-100,200] ms window around
277 the target onset for Exp 1A and more than 70% of missing data points in the
278 [-100,100] ms window around the target onset for Exp 1B, 2A,B and 3, or with

279 more than 60% of missing data points overall (for all experiments), were
280 automatically excluded from the pre-processing pipeline. ANEMO was used to fit a
281 piecewise linear and non-linear model to individual trials' eye velocity to extract the
282 relevant oculomotor parameters (see **Figure 1e** for an illustration of the model
283 fitting and extracted parameters). The model comprised a linear baseline phase (flat
284 linear regression), and two non-linear phases: an anticipatory phase modeled by an
285 exponential function and a visually-guided phase modeled by a sigmoid function.
286 Importantly, we selected this model after comparing its performance quantitatively
287 (using AIC, BIC and RMSE indicators of goodness of fit) with a more standard
288 piecewise linear model (implemented in ANEMO): in all experiments our model
289 (linear + non-linear model) performed better than the linear one in the large
290 majority of trials. In Experiment 1A, the fit was performed in the time window of
291 -300 to 350 ms relatively to the target motion onset. In Experiments 1B, 2A,B and 3,
292 the fit was performed in the time window of -300 to 300 ms relatively to the target
293 motion onset. The relevant model-fit parameter for this study was only the
294 maximum velocity of the anticipatory phase (aSPv), calculated as the maximum
295 value of the exponential function (i.e. its value at the offset of the anticipatory
296 phase). Other oculomotor parameters are automatically extracted by the ANEMO
297 toolbox, but we do not report them in the present study.

298 Eye velocity traces and model fits were visually inspected to exclude the
299 remaining aberrant trials and those with extremely poor fits. Overall, 12% of the
300 trials were excluded on average for Experiment 1A (median: 10%, max: 18%), 16%

301 for Experiment 1B-2A (median: 14 %, max: 32%), 13 % for Experiment 2B (median:
302 13 %, max: 15 %), and 26 % for Experiment 3 (median: 25 %, max: 33 %).

303 **Data analysis**

304 In all experiments, when analyzing the effects of the probability bias, the first
305 10 trials of each block were excluded from analysis. This was done in the aim of
306 excluding large fluctuations related to learning the stimuli statistics and focus on
307 average values rather than on their rate of change. For control, we also repeated all
308 analyses excluding the first 50 trials: the results did not change significantly.

309 Linear Mixed Effects regression Models (*nlme* package for R) were used to
310 evaluate the effects of the target kinematics (different constant speed and
311 acceleration conditions) and of the kinematic probability on the anticipatory smooth
312 pursuit velocity (aSPv) estimates. Because not including a true random effect can
313 increase the false positive rate (Barr et al., 2013), participants were treated as a
314 random effect and all fixed effects were allowed to vary with it. Since this approach
315 usually leads to models that don't converge because of the high number of
316 parameters and the correlations between them, when needed, we used the *buildmer*
317 package for R (Voeten, 2020) to find the maximal model (i.e., the model including
318 the most of variables) which still converges for the dependent variable. After finding
319 the models, we fitted the data and result tables were exported with the *stargazer*
320 package for R (Hlavac, 2022).

321 For Experiment 1A, the models included only speed probability as a fixed
322 effect for the oculomotor anticipatory velocity (aSPv). We chose to use the
323 probability of the highest speed, P(HS), as the independent variable in the model 1:

$$324 \quad (1) \quad aSPv \sim 1 + P(HS) + (1 + P(HS) \mid participant)$$

325 The variable before the \sim symbol is the dependent variable, and the variables
326 after it are the independent variables (also called fixed effects). The 1 corresponds
327 to the model intercept. For the variables within the parentheses, each one before the
328 \mid symbol is allowed to vary for each level of the variable after it (also called random
329 effect). In other words, for each participant, the model will return a different best-fit
330 value for the intercept and the slope of the linear dependence upon probability. For
331 the analysis of the probability-mixtures of Experiment 1B % (v11c vs v33c) and
332 Experiment 2 (v11a vs v33d), we also added the axis (horizontal/vertical) as an
333 interaction factor with the probability, given that the target moved along one of the
334 diagonals. For Experiment 2, we included an interaction with the experiment
335 (2A/2B). The final models, as well as the statistics tables are presented in the
336 supplementary material.

337 It is known that recent trial-history can affect the behavior in the present trial
338 (sequential effect), and this could be seen as a confound in our analyses addressing
339 the effect of the target motion probability across several trials. Therefore, we re-ran
340 the regression models for Experiments 1A and 1B adding the target velocity at trial
341 N-1 (Tv_{N-1}) as an interaction variable:

$$342 \quad (2) \quad aSPv \sim 1 + P(HS)*Tv_{N-1} + (1 + P(HS) + Tv_{N-1} \mid participant)$$

343 In Experiment 3, considering that each target kinematic condition could be
344 uniquely identified as a combination of an initial velocity and acceleration values,
345 we ran a second linear mixed-effects regression model: this time the main
346 independent variables were the target initial velocity ($v0$: 11, 22, or 33°/s) and the
347 target acceleration ($accel$: 0, +22 and -22°/s²), as well as their interaction, all treated
348 as parametric variables:

$$349 \quad (2) \quad aSPv \sim 1 + v0*accel + (1 + v0 + accel | participant)$$

350 In order to test the actual role of target acceleration this model was tested
351 against the model including only $v0$ as fixed effect using the *bayestestR* package for
352 R (Makowski et al., 2019). Pairwise comparisons between $aSPv$ corresponding to the
353 target kinematics (Tk) conditions of Experiment 3 were based on a categorical LMM,
354 initially defined as:

$$355 \quad (3) \quad aSPv \sim 1 + Tk + (1 + Tk | participant)$$

356 Contrasts between the different conditions were performed using the
357 *emmeans* package for R (Lenth, 2017) and p-values were adjusted for multiple
358 comparisons using the Benjamini & Hochberg method for controlling the false
359 discovery rate.

360 We then tested the hypothesis that anticipatory eye velocity is driven by an
361 estimate of the mean target velocity across a finite *temporal window of integration*
362 (TWI) starting at target motion onset (time 0) and ending at time TWI^{end} . In order to
363 do so we fitted, for the pooled participants' data, the following linear regression:

364 (4) $aSPv = slope * Tk + intercept$

365 and extracted the individual best-fit value for the parameters $slope_i$ and
366 $intercept_i$. Here, Tk included $v11c$, $v22c$, and $v33c$. We then used the same relation
367 (5) for the six conditions with accelerating targets, indexed by the suffix i , replacing
368 Tk by the target speed estimate (TSE_i), which approximates the accelerating
369 kinematics:

370 (5) $aSPv_i = slope * TSE_i + intercept$

371 Solving with respect to TSE_i we have:

372 (6) $TSE_i = (aSPv_i - intercept) / slope$

373 By imposing the equality between the estimated target speed TSE_i and the mean of
374 the accelerating/decelerating target speed over a finite TWI, between 0 and TWI^{end} ,
375 we obtain:

376 (7) $(aSPv_i - intercept) / slope = 1/TWI^{end} \times \int_0^{TWI^{end}} (v0 + a * t) dt$

377 where a is the acceleration value and $v0$ the initial target speed for accelerating
378 conditions. Finally, by solving Equation 8 with respect to TWI^{end} we could estimate,
379 for each acceleration condition, the final point in time of the temporal window of
380 integration,

381 (8) $TWI^{end} = 2/a \times [(aSPv_i - intercept) / slope - V0]$

382 In order to have a robust estimate of the variability of such temporal window of
383 integration across the population, we used the bootstrapping technique ($n=1000$,
384 Efron, 1979) and extracted the 95% confidence interval around the mean estimated
385 TWI^{end} .

386 Results

387 Effects of target speed probability on anticipatory Smooth Eye 388 Movements

389 Using a state-of-the-art eye movement recording technique (scleral search
390 coil), we first investigated the effects of target speed probability upon anticipatory
391 smooth eye movements. In Experiment 1A, three participants had to smoothly
392 pursue a target which moved rightwards along the horizontal axis with two
393 different possible speeds (referred to as high-speed, HS, and low-speed, LS)
394 randomly interleaved across trials but with a given probability of occurrence ($P(\text{HS})$
395 and $P(\text{LS}) = 1 - P(\text{HS})$) within a block. **Figure 2a** shows the trial-averaged eye velocity
396 curves for one participant, sorted by probability and target speed conditions. Each
397 probability condition is represented by a different color. The two different target
398 speed profiles are illustrated by the horizontal dotted lines; time zero corresponds to
399 target motion onset. Participants were able to track the two target motions with
400 high accuracy, as shown by the convergence of eye velocity to the target speed
401 during steady-state pursuit. Since target motion direction was always rightward, we
402 observed a strong anticipatory response for all speed probability conditions, as
403 evidenced by the non-zero eye velocity at the usual pursuit latency in humans

404 (~100 ms). However these anticipatory responses in the predicted direction were
405 also modulated by target speed probability. We analyzed such modulation by
406 considering the relationship between amplitude of anticipatory responses and
407 P(HS), i.e., the probability of the highest speed (16.5 °/s). As illustrated in **Figure**
408 **2a**, higher values of P(HS) drove stronger anticipatory pursuit, regardless of the
409 actual target speed (16.5 ou 5.5 °/s). **Figure 2b** plots the relationship between mean
410 anticipatory eye velocity (aSPv) and P(HS), for the 3 participants. The gray curves
411 are the linear relationships estimated from the Linear Mixed Effects Model (LMM).
412 We found a clear linear dependency of anticipatory response upon the probability of
413 target speed, in the direction of target motion. The LMM statistical analysis (with
414 P(HS) as a fixed effect) shows that aSPv significantly increased with higher
415 probability (P(HS) effect: $\beta = 3.48$, 95% CI = (3.14,3.84), $p < .001$). Overall,
416 anticipatory responses were stronger by ~200 %, rising from 2.5 to 7.5 °/s when
417 P(HS) increased from 0 to 1.

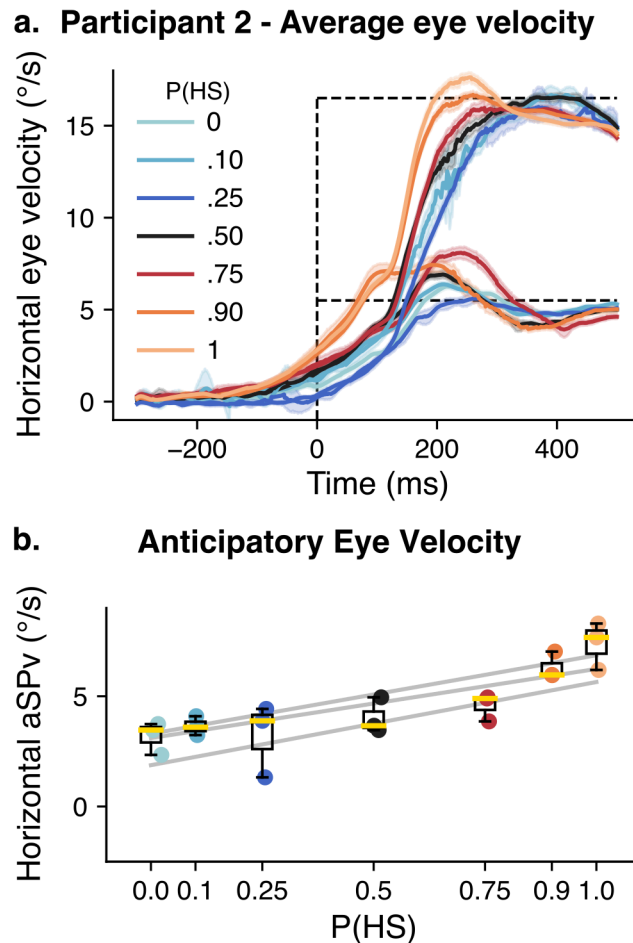


Figure 2. Experiment 1A: Dependence of anticipatory eye velocity upon target speed probability. **(a).** Average eye velocity as a function of time (\pm 95% confidence interval) for one representative participant. Trials are grouped by probability of the higher speed (HS). Each color corresponds to one probability condition. The time zero corresponds to the target onset, and the dashed lines indicate the two possible target speeds. **(b).** Anticipatory eye velocity for the group of participants. Each box plot (median in yellow, box limits corresponding to the 25% and 75% quartiles, and whiskers corresponding to 1.5 times the interquartile range, IQR) corresponds to one probability condition. The gray lines show the linear mixed model fit for each participant.

418 In a second version of this Experiment (Exp 1B), our objective was to
419 replicate the speed-probability dependency of anticipatory pursuit on a larger group
420 of 13 participants, with a less invasive eye tracking technique. We used two new

421 speeds (11 and 33°/s) and a reduced set of probability conditions in the mixture
422 blocks ($P(v_{33c}) = 0, 0.3, 0.7$ and 1). By using an oblique target motion direction, our
423 second objective was to generalize this speed probability dependency across visual
424 motion directions, by having the target moving along one of the 4 diagonal
425 directions (**Figure 1b**). To directly compare the results of Experiment 1A and 1B, we
426 first report the effects of target speed probability observed when varying $P(v_{33c})$ –
427 and therefore $P(v_{11c}) = 1 - P(v_{33c})$ – across blocks with constant speed (v_{11c}, v_{33c})
428 mixtures. **Figure 3a** shows an example of the trial-averaged eye velocity as a
429 function of time for one participant, sorted according to the target velocity profiles
430 (dotted lines) and $P(v_{33c})$ values. Horizontal dotted lines depict the target
431 horizontal and vertical velocity components (i.e. 7.77 and 23.3 °/s for 11 and 33 °/s
432 radial speed). A comparison with **Figure 2a** shows a behavior similar to Exp 1A
433 where target motion was horizontal. Final pursuit velocity matches target velocity,
434 especially for the lowest target speed (v_{11c}). The fact that steady-state eye velocity
435 gain remained lower than 1 for the fastest target speed (v_{33c}) is consistent with
436 previous studies (Carl & Gellman, 1987; Dodge, 1930). As in Exp 1A, target motion
437 direction remained constant within a block, thus a robust anticipatory pursuit
438 response was always observed. However, its amplitude increased when $P(v_{33c})$
439 increased. Such dependency is illustrated in **Figure 3b**, where horizontal and
440 vertical components of anticipatory eye velocity (aSPv) are plotted against $P(v_{33c})$.
441 Both components increased linearly with the probability of the highest speed. A
442 symmetric relationship was observed with $P(v_{11c})$. We ran the LMM statistical
443 models for the anticipatory response (aSPv), including the effect of $P(v_{33c})$, as for

444 Exp 1A. We added the effect of the eye velocity axis (horizontal or vertical) and its
445 interaction to test whether aSPv was differently modulated along the horizontal and
446 vertical dimensions. aSPv increased significantly for higher probability of P(v33c)
447 (**Figure 3b**, P(v33c) effect: $\beta = 2.74$, 95% CI = (1.82, 3.66), $p < .001$). We did
448 not find a significant difference (given a criterion of $\alpha < 0.01$) between axes
449 (main axis effect: $\beta = -0.74$, 95% CI = (-1.46, -0.016), $p = 0.046$), but the effect
450 of P(v33c) was significantly smaller in the vertical axis (P(v33c)*axis effect: $\beta =$
451 -0.67 , 95% CI = (-0.98, -0.36), $p < .0001$). Overall, the two experiments strongly
452 support the fact that anticipatory eye velocity scales with the probability of target
453 speed, in a similar way across different motion directions in the plane, although
454 slightly less robustly along the vertical direction.

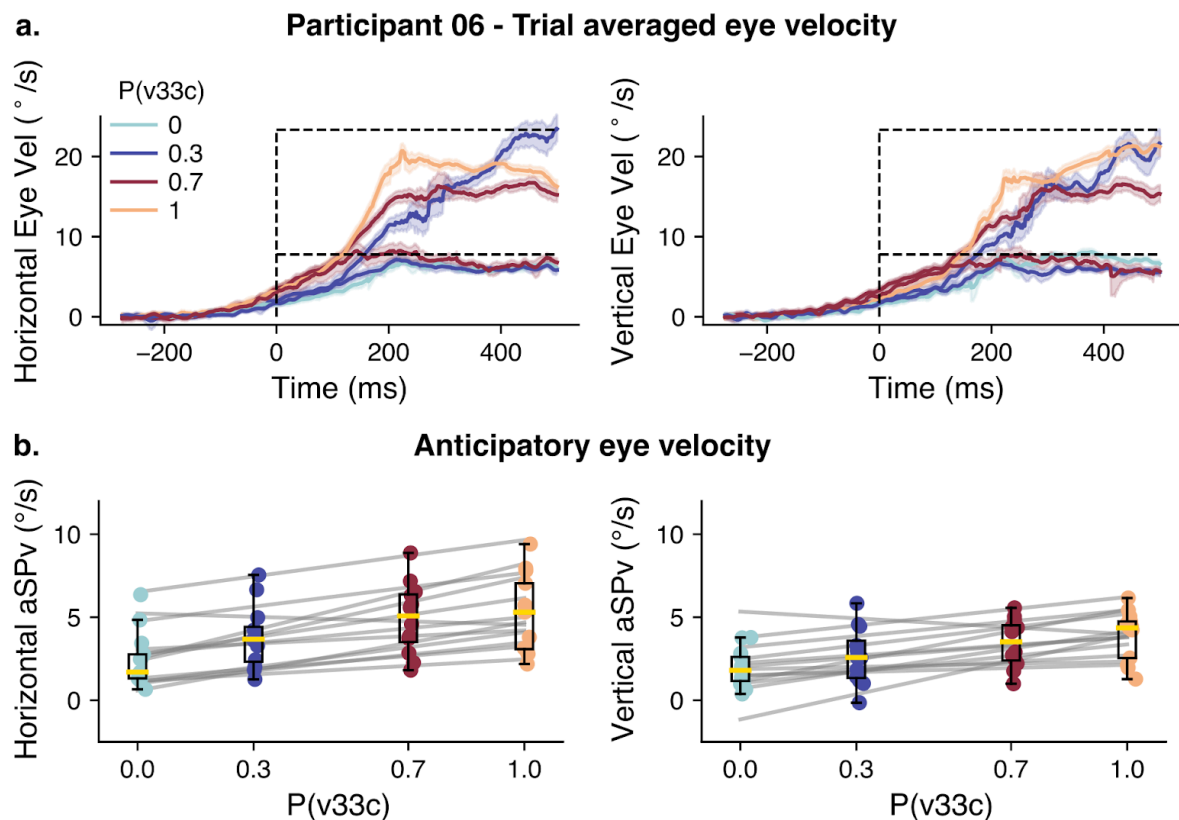


Figure 3. Experiment 1B: Dependence of anticipatory eye velocity upon target constant-speed probability. **(a).** Average eye velocity for trials grouped by probability of v33c and by target velocity for the (v11c,v33c) mix. The left panel shows the horizontal eye velocity, while the right panel shows the vertical eye velocity for a representative participant. Each color corresponds to the different probabilities of v33c. **(b).** Amplitude of anticipatory pursuit is plotted against P(v33c), along the horizontal (left panel) and vertical (right panel) axes. Data represented in the same way as Figure 2.

455 Short and long-time scale factors affecting speed expectation and eye 456 movement anticipation

457 Recent trial history, that is the stimulus properties (e.g. the target speed) observed
458 in the previous trial, or across the few previous trials, can modulate anticipatory eye
459 movements (e.g. Heinen et al., 2005; Kowler & McKee, 1987; Kowler & Steinman,
460 1979; Maus et al., 2015). Importantly, several studies have also shown that both
461 short-term factors related to one or few previous trials, and longer-term factors,
462 related to global statistical estimates can coexist and interact to control perception
463 and visuomotor behavior (e.g. Chopin & Mamassian, 2012; Maus et al., 2015,
464 Damasse et al., 2018; Falmagne et al., 1975; Kowler, 1984; Pasturel et al., 2020; Wu
465 et al., 2021). In order to quantify the effects of the previous trial's speed on the
466 anticipatory eye velocity in the present study, as well as its interaction with the
467 block's speed probability, we ran a new LMM, now including both the
468 speed-probability and the target speed at the trial N-1 (Tv_{N-1}). Note that our study
469 was not designed specifically to study sequential effects (i.e., by presenting all
470 possible combinations of N-1, N-2, N-3,... trials), and therefore we limit our analysis
471 of short-term effects only to the effect of the trial N-1. When the previous trial was a
472 low-speed trial, aSPv decreased when compared to a previous high-speed trial

473 (Exp1A: beta = -0.50, 95% CI = (-0.66, -0.34), $p < .001$; Exp1B: beta = -0.61, 95%
474 CI = (-0.88, -0.34), $p < .001$). For both Experiment 1A and 1B, we found that the
475 main effect of target speed probability upon aSPv remained significant (Exp1A,
476 $T_{V_{N-1}=HS}$: beta = 4.35, 95% CI = (3.98, 4.72), $p < .001$; Exp1B, $T_{V_{N-1}=v33}$: beta =
477 1.38, 95% CI = (0.44, 2.32), $p < 0.01$). The interaction between the previous trial's
478 speed and the block's speed probability was also significant, although with a
479 different sign: for Experiment 1A the probability effect was reduced when the
480 previous trial was low-speed compared to high speed (beta = -2.74, 95% CI =
481 (-3.10, -2.38), $p < .001$); in contrast, for Experiment 1B the probability effect
482 increased when the previous trial was at v11c compared to v33c (beta = 0.82, 95%
483 CI = (0.38, 1.26), $p < .001$). These results are illustrated in the left panels of **Figure**
484 **4a,b**. In the right panels of **Figure 4a** and **4b** we plotted, for Experiment 1A and 1B
485 respectively, the difference between the mean aSPv for trials following a high-speed
486 (in red) or a low-speed (in blue) trials and the mean aSPv across all trials in a
487 probability block. This illustration allows us to immediately capture how the N-1
488 trial's effect is modulated across the probability values: a high-speed previous trial
489 has a larger excitatory impact on subsequent anticipatory velocity when high-speed
490 trials are less frequent. The symmetric interaction is observed for a low-speed
491 previous trial, namely its inhibitory effect is stronger in blocks with a low
492 probability of low-speed trials.

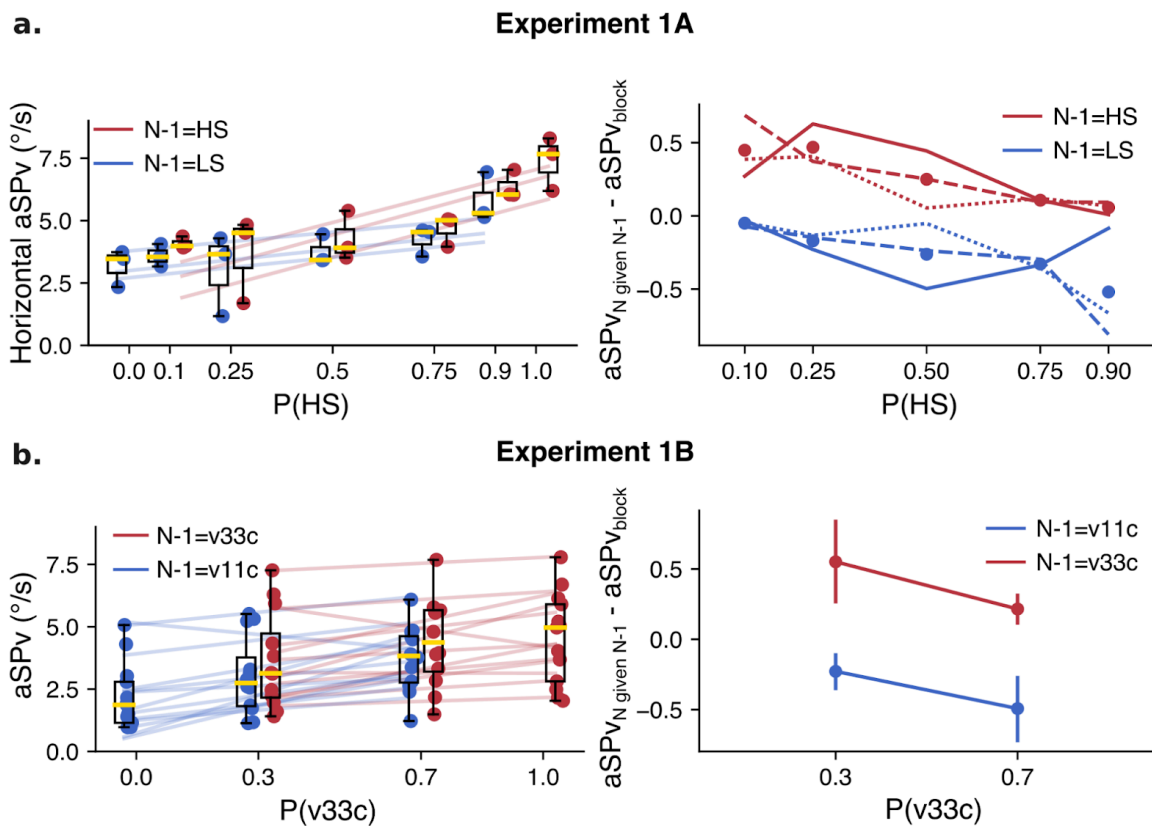


Figure 4. Effect of previous trial's speed versus block's probability. **(a) Experiment 1A.** The left panel shows the probability effect on the aSPv given that the trial N-1 was a high-speed trial (HS, red) or a low-speed trial (LS, blue). The right panel shows the difference between the mean aSPv for trials with N-1 = HS (red), or N-1 = LS (blue) and the mean aSPv in the whole block. Each trace corresponds to one participant, while dots correspond to the average between participants. **(b)** Same analysis for Exp 1B. On the right panel, individual traces were substituted by the 95% confidence interval across participants for the sake of clarity.

493 Effects of the accelerating target probability on anticipatory eye 494 movements

495 Following the same reasoning as for constant speed mixture blocks, we tested
496 the effect of the probability of accelerating target kinematics on aSP. In Experiments
497 2A and 2B, we compared different probabilistic mixtures of trials of accelerating or
498 decelerating target motion. Participants ran blocks of 4 different probability pairs

499 $(P(v33d), P(v11a))$: (0,1), (0.3, 0.7), (0.7, 0.3) and (1,0). In Figure 5, we present the
500 results relative to $P(v33d)$ values. Figure 5a shows horizontal and vertical
501 trial-averaged eye velocities for one participant and each available combination of
502 $P(v33d)$ and target kinematic conditions. Again, each color depicts one probability
503 condition and time zero indicates the target movement onset. We can see clear
504 anticipatory responses, with stronger anticipation occurring for higher probabilities
505 of the highest initial velocity and decelerating motion. After the anticipatory phase,
506 eye velocity traces corresponding to v_{acc} or v_{dec} trials separate and converge to the
507 target's velocity which keeps changing in time according to the acceleration
508 condition. Notice that the anticipation seen with $P(v33d)=0$ (i.e., $P(v11a)=1$) was
509 particularly small but still significant in participant 6, as in all others. Figure 5b
510 plots the horizontal and vertical aSP_v , as a function of $P(v33d)$, for all participants.
511 There is an increase in the amplitude of anticipatory pursuit as $P(v33d)$ increases, as
512 confirmed by the LMM statistical analysis ($P(v33d)$: $\beta = 1.88$, 95% CI = (1.11,
513 2.65), $p < .001$). Consistently with the previous analysis, we did not find any
514 significant difference between axes (axis main effect: $\beta = -0.46$, 95% CI =
515 (-1.26, 0.34), $p = 0.26$) and the interaction between axis and probability did not
516 survive the model selection procedure, suggesting it was not significant. We found
517 that the aSP_v was slightly higher in Exp 2B (constant target duration) than in Exp
518 2A (constant target displacement) (experiment effect: $\beta = 1.68$, 95% CI = (1.41,
519 1.95), $p < .001$), but, again, the interaction between experiment and probability was
520 excluded from the selected model. Overall, in the probability-mixture blocks with
521 accelerating targets, we observed a robust probability-dependent anticipation,

522 similar to the mixture blocks with constant speed and this regardless of the motion
523 direction. The significant main effect of the experimental design (difference between
524 Exp 2A and 2B) suggests that the temporal regularity across trials generally favors
525 anticipatory behavior; however, the lack of interaction between the experiment
526 design and the probability effect argues against a critical role of the motion
527 presentation duration (at least in the tested range, namely above 500ms) on the
528 integration of information about the target acceleration.

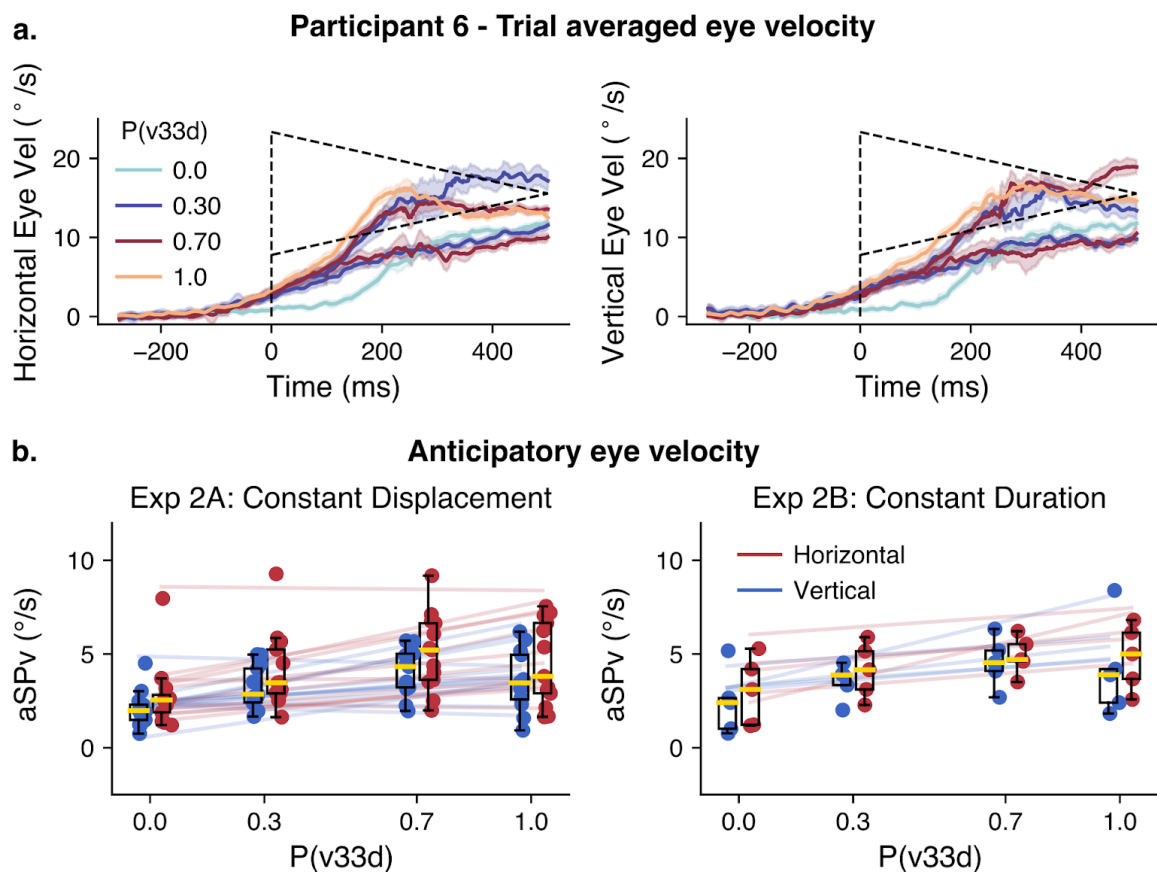


Figure 5. Experiment 2A,B. Effect of the probability of accelerating target kinematics upon anticipatory eye movements (mixture blocks). **(a).** Average eye velocity across time for a representative participant. Trials are grouped according to the probability of v33d (P(v33d)) and sorted by the different target kinematic conditions for each (P(v33d), P(v11a)) mixture. Left and right panels show horizontal and vertical eye velocity profiles, respectively. The dashed lines show the target velocity. **(b).** Mean anticipatory eye

velocity as a function of the probability of v33d, group results. The left panel shows the data for Exp 2A, while the right panel shows the data for Exp 2B. Horizontal data is shown in red, and vertical data is shown in blue. Data represented in the same way as Figure 2.

529 Effects of different target kinematics on anticipatory Smooth Eye 530 Movements

531 Lastly, we questioned in Experiment 3 how the anticipation for accelerating
532 target motion compares to that observed for constant target speeds. We compared
533 three conditions where oblique target motion had a constant speed (v11c, v22c and
534 v33c, corresponding to radial 11, 22 and 33 °/s, respectively) to conditions in which
535 the target started at 11, 22 or 33 °/s and either accelerated uniformly (v11a, v22a,
536 v33a, acceleration = 22 °/s²) or decelerated uniformly (v11d, v22d, v33d,
537 acceleration = -22 °/s²). The different target kinematic conditions were presented in
538 a block design and motion direction was fixed for each participant, leading to full
539 predictability of both target's trajectory and kinematics (P = 1). **Figure 6** shows eye
540 velocity profiles recorded in one participant, for Exp 3, for each target kinematic
541 condition illustrated by the dotted lines. Each row of **Figure 6** corresponds to one
542 initial target speed value, while acceleration values are shown in different colors
543 (accelerating motion in green, constant motion in blue, and decelerating motion in
544 pink). Predictable constant speed targets drove strong anticipatory pursuits that
545 were scaled according to target speed (blue curves, from top to bottom). Moreover,
546 accelerating conditions also resulted in clear anticipatory pursuit responses. As
547 clearly seen with the 22 and 33°/s initial speed conditions, green and red curves are,

548 respectively, above and below the blue ones, illustrating that anticipatory responses
549 were modulated by both initial speed and target acceleration.

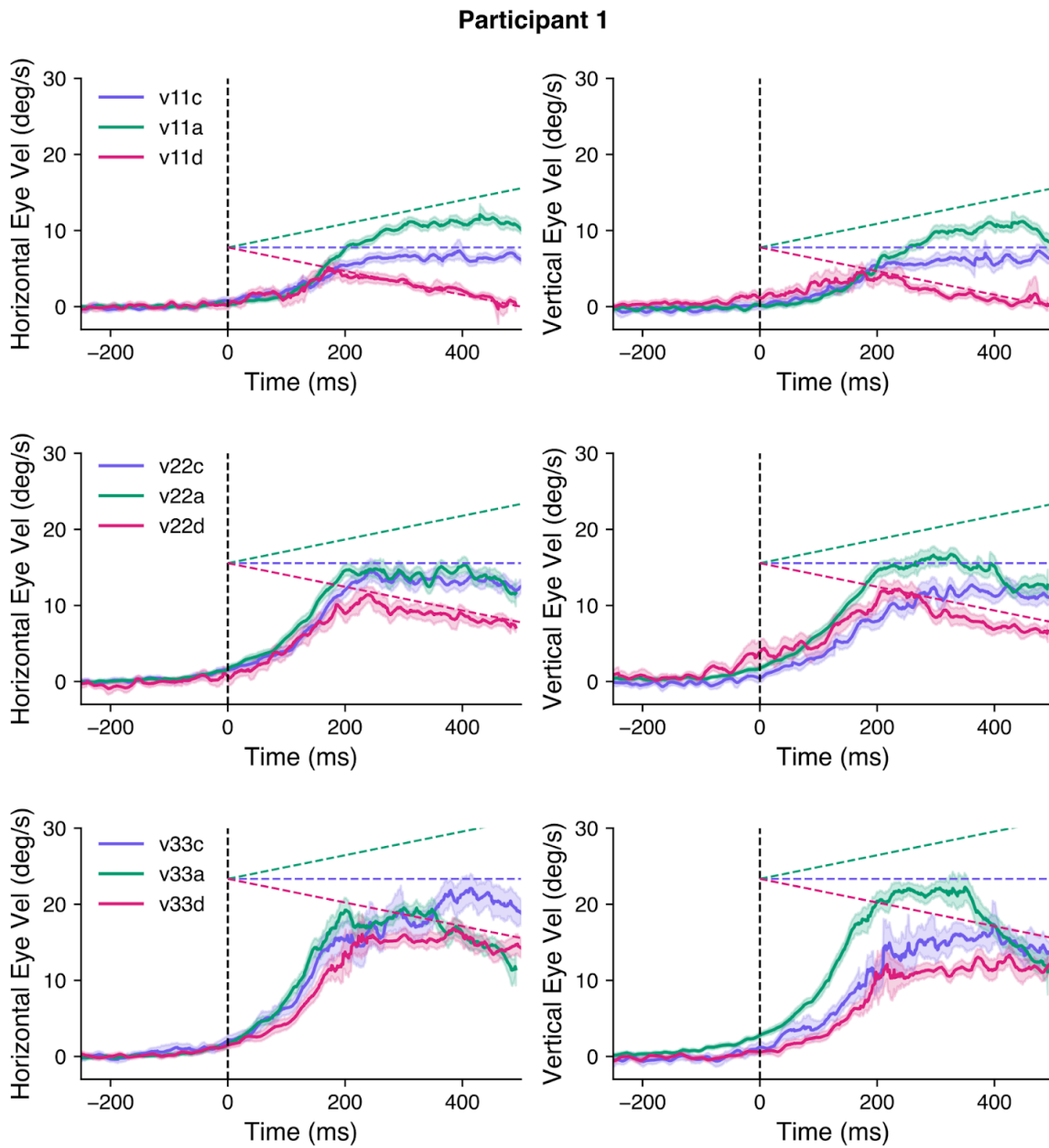


Figure 6. Experiment 3: Effect of target kinematics on aSP (fully predictable blocks). (a). Average eye velocity over time with trials grouped by target speed (rows: v11, v22, and v33 from top to bottom) and target acceleration values (color coded: accelerating in green,

constant in blue, decelerating in pink) for one participant of Exp 3. The dashed lines show the corresponding target speed profile for each acceleration value.

550 **Figure 7** illustrates the amplitude of anticipatory pursuit responses (aSPv) for
551 the different conditions across all participants. Note that, for each initial speed,
552 there is a tendency for aSPv to increase as the acceleration increases. To statistically
553 test the effect of acceleration on the anticipatory eye velocity, we ran a parametric
554 linear mixed-effects regression model including both the acceleration and the initial
555 target speed as independent variables.

556 We found that a model including both the initial speed and acceleration was
557 significantly better than a model including only the initial speed (speed-only model
558 BIC = 43521.6; full model BIC = 43308.97; Bayes Factor = $1.48e + 46$). The initial
559 speed significantly modulated the aSPv (v_0 : beta = 0.24, 95% CI = (0.15, 0.34),
560 $p < .001$), while the acceleration alone had a significant but smaller positive effect
561 on the aSPv (accel: beta = 0.017, 95% CI = (0.004, 0.030), $p = 0.009$), indicating
562 that indeed aSPv increases with target acceleration. We also found a significant
563 positive interaction between initial speed and acceleration ($v_0 * \text{accel}$: beta = 0.001 ,
564 95% CI = (0.0004, 0.002), $p = .004$), indicating that the effect of acceleration is
565 stronger for high initial speeds when compared to low initial speeds.

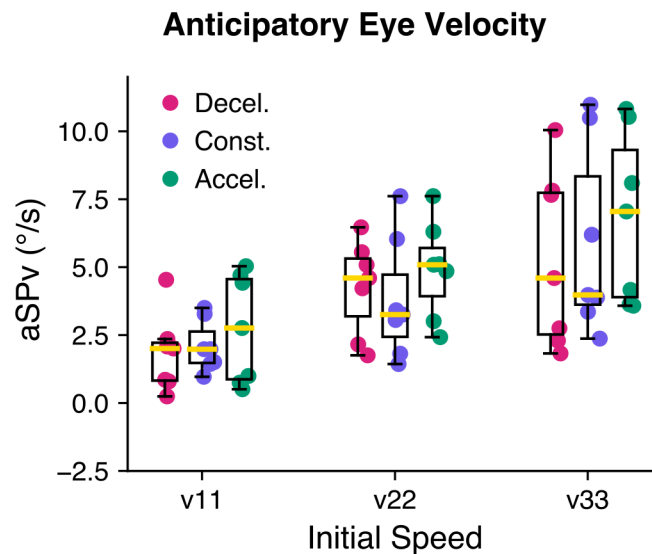


Figure 7. Experiment 3: Group effect of target kinematics on the aSPv. aSPv is grouped by initial velocity (v11, v22 and v33, from left to right, respectively) and acceleration values are shown in different colors (decelerating target motion in pink, constant target motion in blue and accelerating target motion in green). Data are represented in the same way as Figure 2.

566 Temporal window of estimation of the mean target speed for accelerating 567 motion

568 Previous studies investigating predictive smooth pursuit during the transient
569 disappearance of the target have compared different possible schemes of temporal
570 integration to build an internal model of complex target motion. Such alternative
571 internal models could either take into account only the last sample of observed
572 target velocity before target blanking, or an average of velocity across a finite time
573 window, or use both the last velocity sample and its rate of change. Their results
574 suggest that the rate of speed change (i.e. acceleration) was only taken into account
575 if target displacement properties were estimated during a sufficiently long interval

576 (Bennet et al. 2007). Performance was in any case inaccurate due to a lack of
577 sufficient extrapolation of accelerating motion (Bennet & Benguigui 2013). Together
578 with the results of Bennet and Barnes (2006), our results suggest that the target's
579 acceleration is integrated, though with a small weight and large variability, in the
580 internal model of visual motion that drives anticipatory smooth eye movements
581 across a block of trials where the target motion is highly predictable (as illustrated
582 in the previous section). However, such an effect does not imply, *per se*, that a
583 representation of target acceleration is accessible to the visuo-motor system. For
584 instance, an estimate of target speed across a finite temporal window could be used
585 as a proxy for target motion and drive anticipation. Thus, we simulated a similar but
586 more realistic version of the simplest, initial speed based, internal model of target
587 motion. We reasoned that, rather than an instantaneous estimate of target velocity
588 (in our case the target velocity at time 0, or target motion onset) the internal model
589 of motion stored in memory would take into account an estimate of the mean target
590 velocity computed over a finite time-window around target motion initiation. This
591 alternative model could accommodate the observation that expectancy-based
592 anticipatory velocity differs, but only weakly, for two targets with the same initial
593 velocity and a different acceleration. Note that we can already speculate that such
594 hypothetical temporal window of integration should be shorter than 500ms. If this
595 was not the case, aSPv should not differ between target kinematic conditions that
596 lead to the same mean target speed across the 500ms window of motion
597 presentation. In Experiment 3, two pairs of conditions fit to this requirement,
598 namely (v11a, v22d) and (v22a, v33d). For both pairs, aSPv is significantly higher

599 for the second than for the first target kinematic condition ($v11a-v22d = -1.503$, SE
600 $= 0.139$, $p < .0001$; $v22a-v33d = -0.443$, SE $= 0.132$, $p < .001$).

601 **Figure 8** illustrates the rationale and the results of our model-based analysis of the
602 temporal window of velocity integration. We have shown in the previous sections
603 that a linear regression describes the relationship between target speed and
604 anticipatory eye velocity for predictable, constant target speeds (schematically
605 illustrated in **Figure 8a**, upper panel, blue line). We assumed that 1) the same linear
606 regression applies to the accelerating conditions as well, to describe the relationship
607 between anticipatory eye velocity and the target speed estimate (TSE)
608 approximating the accelerating kinematics; 2) such an estimate, TSE, would
609 correspond to the mean target speed computed over a finite temporal window of
610 integration (TWI), starting at time 0 (target motion onset) and ending at time
611 TWI^{end} . Thus, in order to have a reliable estimate of TWI^{end} for all kinematic
612 conditions across participants, we first estimated the linear regression between aSPv
613 and target speed at the group level, by pooling the data of all participants together.
614 We then computed the mean TSE knowing the aSPv values corresponding to
615 accelerating conditions and inverting the above-mentioned linear relation (as
616 illustrated in the top panel of **Figure 8a**). From the TSE value, we finally inferred
617 the mean TWI^{end} (as schematized in **Figure 8a**, bottom panel) and its variability
618 using a bootstrapping procedure (Efron, 1979, see **Figure 8b**; for details of the
619 calculations please refer to the figure caption and the Methods section). Note that
620 the estimated TWI^{end} for accelerating conditions is between 0 and 500 ms, although
621 the distribution is very broad ($v11a$, mean $= 0.15$, 95% CI $= (-0.04, 0.34)$; $v22a$,

622 mean = 0.18, 95% CI = (-0.03, 0.33); v33a, mean = 0.19, 95% CI = (-0.14,
623 0.49)). Remarkably, the TWI^{end} distribution for decelerating conditions displays
624 smaller values, largely overlapping with 0, but also includes a wide range of
625 unrealistic (negative) values (v11d, mean = -0.01, 95% CI = (-0.17, 0.10); v22d,
626 mean = -0.09, 95% CI = (-0.23, 0.07); v33d, mean = 0.004, 95% CI = (-0.33,
627 0.32)).

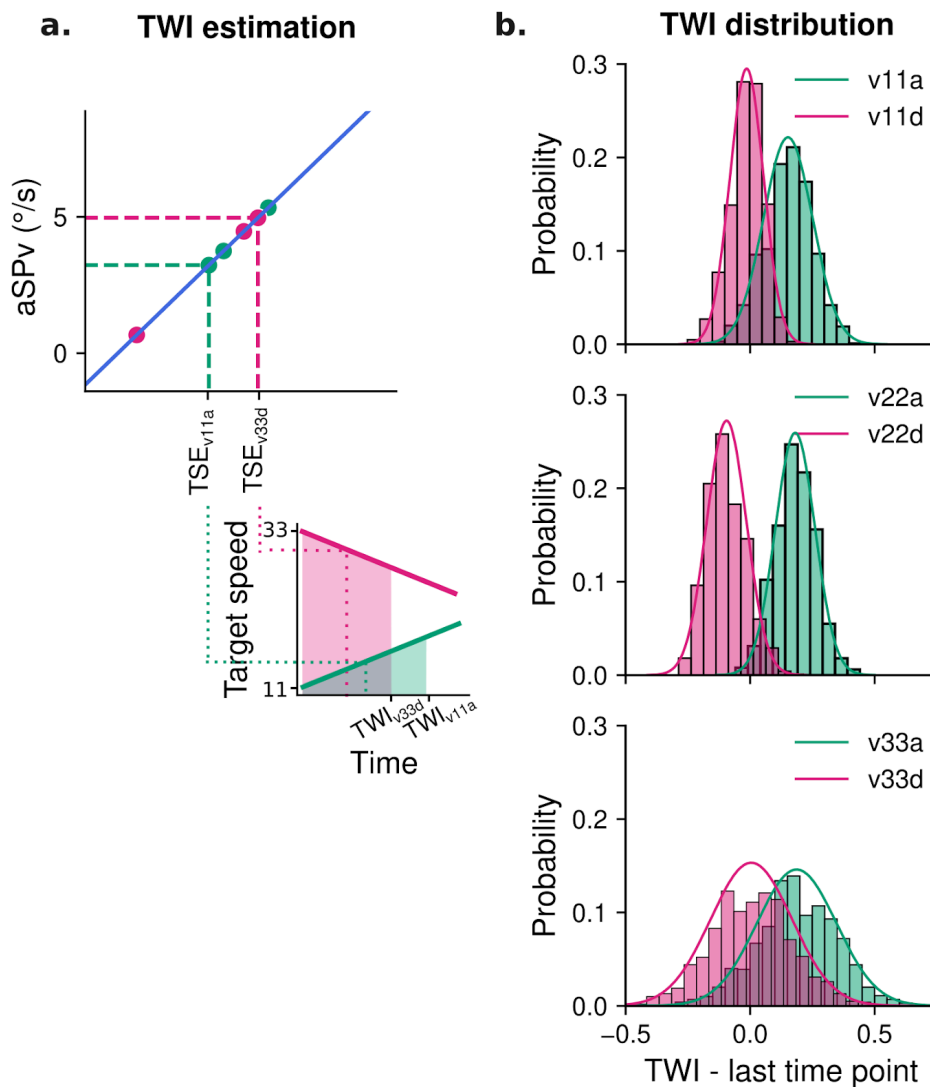


Figure 8. Testing the hypothesis of a finite temporal window of integration (TWI) to extract a target speed estimate (TSE) for accelerating conditions. (a) Schematic

illustration of the procedure to compute the temporal window (the number of datapoints is reduced, for the sake of clarity: for details refer to the Methods section). **Upper panel:** At the group level and for the constant speed blocks, we calculated the linear regression between aSPv and target speed (blue straight line). On the basis of this regression, for accelerating blocks (pink or green dots), we performed the inverse operation to calculate the estimated target speed (TSE) that would have elicited the observed aSPv. **Lower panel:** The TWI is estimated as the temporal window over which the mean of the accelerating target speed equals TSE, as exemplified for two particular accelerating conditions (v11a and v33d). **(b)** Distribution of the bootstrapped estimates of TWI for the accelerating conditions. Each panel shows the TWI distributions for one initial speed (v11, v22 and v33 from top to bottom) and for the accelerating (pink) vs decelerating (green) target motion. The smooth line depicts a gaussian fit of the histograms.

628 Overall, these results cannot exclude the possibility that visual accelerating
629 motion is approximated by the mean target speed estimate across a finite time
630 window. However, the large variability of the inferred TWI and the presence of
631 incoherent results, like negative TWI^{end} (especially for deceleration targets) impose a
632 strong caution in the interpretation. We will further discuss this finding in the
633 Discussion section.

634 Discussion

635 We had two main objectives with the present study. First, we wanted to analyze the
636 effects of a parametric change of the target speed probability upon human
637 anticipatory smooth eye movements. We have done this by re-analyzing previously
638 collected data (see Souto et al., 2008) and by replicating and generalizing those
639 results in a larger group of participants and different conditions, including targets
640 with different motion direction, speed and acceleration profiles. We used target
641 motion trajectories along both horizontal and oblique directions but kept target

642 motion direction constant within blocks in all experiments. Second, we compared
643 different fully predictable target kinematics, namely constant or accelerating target
644 speeds and analyzed their effect on anticipatory eye movements. We found that
645 anticipatory responses were strongly modulated by both constant and accelerating
646 target speeds. We report a linear scaling of anticipatory smooth pursuit with target
647 speed (or acceleration) probability, similar to what we previously reported for a
648 probability bias in direction and distinct from the short-term trial history effects. We
649 also investigated, through statistical and model-based analyses, whether the internal
650 model of visual motion that drives anticipatory smooth pursuit would integrate
651 information about the target's accelerating profile. Our results, although very
652 variable across participants, provide evidence that humans can integrate some
653 information about acceleration and use it to anticipate the forthcoming target
654 motion. Whether this integration is grounded on an internal, noisy representation of
655 motion acceleration, or on an approximation of the target mean velocity over an
656 extended temporal window remains to be further investigated.

657 **A linear dependence between anticipatory pursuit and the probability of** 658 **target kinematic cues**

659 In two separate experiments, we showed that the velocity of anticipatory
660 pursuit is modulated by the constant-speed probability of visual moving targets,
661 regardless of its fully predictable direction. These results are consistent with
662 previous reports (as reviewed in Kowler et al., 2019) that showed that anticipatory
663 smooth velocity is modulated by the predictability of target speed, as well as by

664 short-term trial-sequence effects. Our results are however novel in several aspects.
665 First, we demonstrate a parametric, linear relationship between the amplitude of the
666 anticipatory phase and a broad range of target speed probability. Such a linear
667 relationship is observed also over a large interval of target speeds (from 5 to above
668 $30^\circ/\text{s}$) and is similar for targets moving along either the horizontal (**Figure 2**) or the
669 oblique axes (**Figure 3**). In addition, similar to a previous study of our group
670 (Damasse et al., 2018) we have provided evidence that short-term effects driven by
671 the previous trial's speed can coexist and interact with the long-term effects that
672 were the main objective in the present study. In particular, experiencing a high
673 (low) speed trial yields an increase (decrease) of aSPv in the following trial with
674 respect to the block's average (**Figure 4**), but this effect is strongly modulated by
675 the context, namely by the probability of high (or low) speed trials. Moreover, we
676 show that higher order kinematic cues such as acceleration can also modulate eye
677 velocity during anticipatory pursuit, again regardless of the (predictable) target
678 motion direction and such an effect is also modulated by the probability of these
679 higher-order kinematic cues (**Figure 5**).

680 Overall, these novel results extend our previous findings of a linear
681 dependence of the anticipatory eye velocity upon the target direction probability
682 (Damasse et al., 2018; Santos & Kowler, 2017) and further demonstrate that the
683 statistical regularities of different motion properties are efficiently stored in memory
684 and used to drive anticipatory visuomotor control across a timescale of several
685 seconds to several minutes and more. Our results argue for a probabilistic coding of
686 target velocity (direction and speed), and possibly of target acceleration as well. Yet,

687 future work is needed to elucidate whether these aspects of target trajectories are
688 encoded together or separately and by which neuronal populations and
689 computational processes. It is important to notice that the present and most of the
690 previous results demonstrating some degree of sensorimotor adaptation to the
691 statistical regularities in the environment do not imply that probabilities are
692 explicitly learnt and/or represented as abstract concepts in the brain. The very
693 nature of probabilistic coding in the brain is at the heart of important lines of
694 research, and the relation between probabilistic coding and probability-based
695 behavior is not trivial at all. In any case, anticipatory smooth pursuit eye
696 movements appear as an effective behavioral measure to elucidate how direction
697 and kinematic parameters are encoded, together with their uncertainty, to control
698 eye movements.

699 **Is there an internal representation of accelerating target kinematics?**

700 In this study, we also addressed the question of *how* information about
701 accelerating motion could be integrated in the internal model of motion that drives
702 anticipatory eye movements. To do so, we analyzed how predictable accelerating
703 targets affect anticipatory eye velocity compared to constant-speed targets. Target
704 motion conditions were designed such that constant speeds can directly be
705 compared with accelerating conditions: each value of initial speed (11, 22 or 33 °/s)
706 was paired with different acceleration values. The linear mixed-effects regression
707 model indicated that anticipatory eye velocity was not simply scaled based on the
708 instantaneous initial target speed, but also on its acceleration. Moreover, the effect

709 of acceleration increased with the initial speed (see **Figure 7**, and statistical
710 analyses reported in the text). We performed an additional model-based analysis to
711 tease apart the possibility that the internal model driving anticipatory smooth
712 pursuit relies, rather than on an exact representation of target acceleration, on a
713 simple approximation of it, namely the estimation of mean target speed across a
714 finite temporal window close to motion onset. Leveraging on the linear relation
715 between predictable target speed and anticipatory eye velocity, this analysis allowed
716 us to simulate the size of the temporal window of integration and its variability
717 across the group of participants tested in this study (**Figure 8**). Overall, the
718 estimated temporal window of integration was strongly variable across participants
719 and in the case of decelerating targets these estimates were often unrealistic (e.g.
720 negative temporal windows). Interestingly, the distribution of TWI estimates with
721 accelerating targets was clearly different from the one obtained with decelerating
722 targets, and centered on positive and plausible values (i.e. around two-hundred
723 milliseconds after target motion onset).

724 Whether and how the acceleration of moving targets is represented and used
725 by the primate visual tracking system is still unclear (Lisberger & Movshon, 1999),
726 even though target acceleration is a key component of many models of visual
727 target-driven smooth pursuit eye movements (Brostek et al., 2017; Goldreich et al.,
728 1992; Krauzlis & Lisberger, 1994). In humans, several previous studies have
729 attempted to demonstrate a role for acceleration and whether such high-order
730 motion cues can be learned through the history of target motion, on both the short
731 (a few hundreds milliseconds) and medium to long (seconds to minutes and more)

732 timescales. Bennett et al. (2007) showed that when smoothly pursuing an
733 accelerating target which undergoes an occlusion after a short exposition (200 ms)
734 in a random-presentation condition, human participants are not able to adaptively
735 use the acceleration information. Instead, participants seem to store the estimate of
736 a constant velocity and use saccades to compensate for the displacement error
737 between the eye position and the location where the target reappears. Those authors
738 found, however, that after a longer exposure (500-800 ms, comparable to our visual
739 motion duration), smooth pursuit and saccades discriminate between the different
740 acceleration profiles. Still, prediction of the target position at the end of the
741 occlusion was not accurate. Using again the transient target-occlusion paradigm,
742 Bennett & Barnes (2006) probed predictive smooth pursuit of accelerating targets in
743 blocked vs random presentation conditions. They reported two interesting and
744 complementary results: in a blocked-design paradigm (thus with highly predictable
745 motion over a long timescale), anticipatory eye velocity occurring (1) before the
746 target motion onset and (2) before the end of target blanking was scaled to the
747 target acceleration. However, increasing uncertainty about target acceleration, by
748 mixing trials, had canceled such dependency and anticipatory eye movements were
749 no longer distinguishable between acceleration conditions. Other studies came to
750 the same conclusion: on a short timescale acceleration information can be used to
751 somehow control online tracking eye (and hand) movements but not to build robust
752 predictive motor responses to moving targets, or related perceptual judgements
753 (Kreyenmeier et al. 2022). On the other hand, predictability over a longer timescale
754 seems to favor the integration of acceleration information for visuomotor control

755 (Bennett & Barnes, 2006). Our results tend to corroborate the latter claim, with the
756 *caveat* of a large inter-individual variability observed in the anticipatory behavior
757 with predictable accelerating motion.

758 Early psychophysical studies have shown that the mean speed estimated over
759 the stimulus motion duration influences the perceptual discrimination of
760 acceleration (Brouwer et al., 2002; Gottsdanker et al., 1961; Schmerler, 1976).
761 Watamaniuk & Heinen (2003) showed that this is also the case when judging and
762 tracking an accelerated moving target. In addition, the duration of the temporal
763 window during which the target kinematic information is acquired seems to
764 influence the accuracy of acceleration estimation (Bennett et al., 2007). In the
765 present study, our model-based analysis of the temporal window of integration
766 highlighted a large inter-individual variability, as well as a dependence on the
767 acceleration sign, in the timescale that would be relevant to estimate the motion of
768 accelerating targets. Overall, several contextual factors seem to influence the
769 encoding and processing of visual motion acceleration. The precise nature -and the
770 mere existence!- of an explicit representation of visual acceleration in the brain
771 remains to be elucidated.

772 We also need a more complete understanding of how speed and acceleration
773 cues can be integrated through learning sensorimotor contingencies in specific tasks.
774 A very peculiar example is the vertical tracking of a target that changes speed by
775 following the gravity acceleration (Zago et al., 2010). What is being learned in an
776 experimental session (e.g. probabilities of occurrence) versus the entire lifespan (e.g.

777 the law of gravity, or friction, see Souto & Kerzel, 2013), and how this drives
778 anticipatory pursuit responses questions the complex interactions between
779 predictive and sensory information for an optimal tracking behavior.

780 Finally, in addition, in alternative or in parallel to the internal model of the
781 retinal target speed and acceleration, reinforcement learning processes could play
782 an important role in adapting anticipatory eye movements to predictable motion
783 properties. Any combination of retinal position, velocity or acceleration errors could
784 be estimated and eventually minimized over trials, akin to a *cost function*, to
785 improve target visibility and tracking performance. Thus, we can speculate that
786 participants could simply learn by trial and error and adapt their anticipation
787 behavior to rapidly minimize the difference between the eyes and target position
788 and velocity, as well as its change over time. Again, this sort of cost-minimization
789 process remains to be thoroughly tested by future model-based experiments.

790 **Neuronal bases of predictive tracking and processing of different kinematic** 791 **properties**

792 Electrophysiological studies in the non-human primates have provided
793 evidence that a small subpart of the Frontal Eye Fields (FEFsem, slightly ventral
794 compared to the saccadic FEF) is implicated in the control of predictive smooth
795 pursuit (e.g. Fukushima et al., 2002; MacAvoy et al., 1991, see Kowler, 2019 for a
796 review). Darlington et al. (2018) showed that FEFsem firing rate is modulated,
797 before visual motion onset, by the expectations about the target speed. In addition,
798 the speed-context modulation of neuronal activity continues throughout the

799 visually-guided phase of smooth pursuit, and it is stronger when the visual stimuli
800 are less reliable (i.e. at lower contrast), in agreement with Bayesian integration of
801 prior beliefs and sensory evidence. Such integration was also apparent in the
802 oculomotor recordings, with the monkeys' smooth pursuit eye velocity more
803 strongly modulated by the speed context for low-contrast targets. Unfortunately, the
804 authors could not compare the FEF preparatory activity with anticipatory eye
805 velocity, nor did they analyze the smooth pursuit latency dependence on motion
806 expectancy, thereby limiting the possibility to draw some correspondence with our
807 results. A second prefrontal oculomotor field, the Supplementary Eye Fields (SEF) is
808 also involved in the control of predictive smooth pursuit (Heinen & Liu, 1997). For
809 instance, de Hemptinne et al. (2008) showed that the activity of a population of SEF
810 neurons encoded the target direction expectations, as neurons became more active
811 after the presentation of a cue indicating deterministically a target motion in the
812 neuron's preferred direction. The evidence for the neural substrates of predictive
813 pursuit is much sparser in humans: Gagnon et al. (2006) have applied transcranial
814 magnetic stimulation (TMS) pulses to the human FEFsem and SEF regions during
815 visual tracking of sinusoidal target motion. They have reported an enhancement of
816 predictive pursuit when TMS was applied to FEFsem at different epochs, but only in
817 some specific conditions when TMS was applied to SEF. Several questions remain
818 yet unanswered. First, the respective role of FEFsem and SEF in predictive eye
819 movement is still debated. Second, how the different variables of target motion
820 trajectories are encoded and learned is yet to be investigated. Thanks to its fast,
821 block-designed protocol mixing different target motion cues, the present study may

822 inspire future neurophysiological studies in non-human and human primates,
823 focusing on the joint analysis of anticipatory responses and preparatory neural
824 activities in these two prefrontal areas.

825 Our results call for a reevaluation of the role of higher-order motion cues
826 (acceleration/deceleration) in the control and learning of predictive pursuit
827 behavior. There is very little evidence that the primate nervous system encodes
828 visual acceleration explicitly, in the visual or in the oculomotor systems. Lisberger &
829 Movshon (1999) measured MT single neurons' responses to image acceleration, but
830 did not find evidence that those neurons' activity varied with acceleration. They
831 found, however, that the simulated nonlinear readout of a population of MT
832 neurons was correlated to image acceleration (though not to its deceleration).
833 Similarly, Price et al. (2005) found speed tuning in MT single neurons, but not an
834 acceleration or deceleration tuning. However, Schlack et al. (2007) showed that a
835 linear classifier can extract acceleration signals from the MT population response,
836 given that the MT neurons' tuning to speed depended on the acceleration and
837 deceleration contexts of the task. Note, however, that these earlier studies focused
838 mainly on primate area MT while other parietal (MST) and frontal (FEF) cortical
839 areas might contribute to represent complex target motion trajectories and
840 higher-order kinematics. Future work shall elucidate how position, velocity and
841 acceleration cues are jointly or independently encoded across the visuo-oculomotor
842 distributed network, to represent and learn target trajectories for the efficient
843 control of action.

844 **Conclusion**

845 In this study, we showed that when the target speed is predictable, human
846 participants show a linear dependence of anticipatory eye velocity upon the speed
847 probability that is comparable to the dependence found for target direction
848 probability. Moreover, participants also show anticipatory responses adjusted to
849 accelerating target kinematics, and to their probability across-trials. Overall, this
850 study contributes to the broad existing literature about the sensory and cognitive
851 control of eye movements by better characterizing the role of predictive information
852 about the target kinematics.

853

854

855 **Data availability statement**

856 The data and analysis scripts are available (DOI 10.17605/OSF.IO/SYD3T).

857 References

- 858 Barnes, G. R., & Asselman, P. T. (1991). The mechanism of prediction in human
859 smooth pursuit eye movements. *The Journal of Physiology*, 439(1), 439–461.
860 <https://doi.org/10.1113/jphysiol.1991.sp018675>
- 861 Barr, D. J., Levy, R., Scheepers, C., & Tily, H. J. (2013). Random effects structure for
862 confirmatory hypothesis testing: Keep it maximal. *Journal of Memory and*
863 *Language*, 68(3), 255–278. <https://doi.org/10.1016/j.jml.2012.11.001>
- 864 Bennett, S. J., & Barnes, G. R. (2006). Smooth ocular pursuit during the transient
865 disappearance of an accelerating visual target: The role of reflexive and
866 voluntary control. *Experimental Brain Research*, 175(1), 1–10.
867 <https://doi.org/10.1007/s00221-006-0533-4>
- 868 Bennett, S. J., & Benguigui, N. (2013). Is Acceleration Used for Ocular Pursuit and
869 Spatial Estimation during Prediction Motion? *PLoS ONE*, 8(5), e63382.
870 <https://doi.org/10.1371/journal.pone.0063382>
- 871 Bennett, S. J., de Xivry, J.-J. O., Barnes, G. R., & Lefèvre, P. (2007). Target
872 Acceleration Can Be Extracted and Represented Within the Predictive Drive
873 to Ocular Pursuit. *Journal of Neurophysiology*, 98(3), 1405–1414.
874 <https://doi.org/10.1152/jn.00132.2007>
- 875 Bennett, S. J., Orban De Xivry, J.-J., Lefèvre, P., & Barnes, G. R. (2010). Oculomotor
876 prediction of accelerative target motion during occlusion: Long-term and
877 short-term effects. *Experimental Brain Research*, 204(4), 493–504.
878 <https://doi.org/10.1007/s00221-010-2313-4>
- 879 Brainard, D. H. (1997). The Psychophysics Toolbox. *Spatial Vision*, 10(4), 433–436.
- 880 Brostek, L., Eggert, T., & Glasauer, S. (2017). Gain Control in Predictive Smooth
881 Pursuit Eye Movements: Evidence for an Acceleration-Based Predictive
882 Mechanism. *Eneuro*, 4(3), ENEURO.0343-16.2017.
883 <https://doi.org/10.1523/ENEURO.0343-16.2017>
- 884 Brouwer, A.-M., Brenner, E., & Smeets, J. B. J. (2002). Perception of acceleration
885 with short presentation times: Can acceleration be used in interception?

- 886 *Perception* & *Psychophysics*, 64(7), 1160–1168.
887 <https://doi.org/10.3758/BF03194764>
- 888 Carl, J. R., & Gellman, R. S. (1987). Human smooth pursuit: Stimulus-dependent
889 responses. *Journal of Neurophysiology*, 57(5), 1446–1463.
890 <https://doi.org/10.1152/jn.1987.57.5.1446>
- 891 Chopin, A., & Mamassian, P. (2012). Predictive Properties of Visual Adaptation.
892 *Current Biology*, 22(7), 622–626. <https://doi.org/10.1016/j.cub.2012.02.021>
- 893 Collewijn, H., Van Der Mark, F., & Jansen, T. C. (1975). Precise recording of human
894 eye movements. *Vision Research*, 15(3), 447-IN5.
895 [https://doi.org/10.1016/0042-6989\(75\)90098-X](https://doi.org/10.1016/0042-6989(75)90098-X)
- 896 Damasse, J., Perrinet, L. U., & Montagnini, A. (2018). Reinforcement effects in
897 anticipatory smooth eye movements. 18(2018), 1–18.
- 898 Darlington, T. R., Beck, J. M., & Lisberger, S. G. (2018). Neural implementation of
899 Bayesian inference in a sensorimotor behavior. *Nature Neuroscience*, 21(10),
900 1442–1451. <https://doi.org/10.1038/s41593-018-0233-y>
- 901 De Hemptinne, C., Lefèvre, P., & Missal, M. (2008). Neuronal Bases of Directional
902 Expectation and Anticipatory Pursuit. *The Journal of Neuroscience*, 28(17),
903 4298–4310. <https://doi.org/10.1523/JNEUROSCI.5678-07.2008>
- 904 Dodge, R. (1930). OPTIC NYSTAGMUS: III. CHARACTERISTICS OF THE SLOW
905 PHASE. *Archives of Neurology & Psychiatry*, 24(1), 21.
906 <https://doi.org/10.1001/archneurpsyc.1930.02220130024002>
- 907 Efron, B. (1979). Bootstrap Methods: Another Look at the Jackknife. *The Annals of*
908 *Statistics*, 7(1). <https://doi.org/10.1214/aos/1176344552>
- 909 Engbert, R., & Kliegl, R. (2003). Microsaccades uncover the orientation of covert
910 attention. *Vision Research*, 43(9), 1035–1045.
911 [https://doi.org/10.1016/S0042-6989\(03\)00084-1](https://doi.org/10.1016/S0042-6989(03)00084-1)
- 912 Falmagne, J.-C., Cohen, S. P., & Dwivedi, A. (1975). Two-choice reactions as an
913 ordered memory scanning process. *Attention and Performance V*, 296–344.
- 914 Fukushima, K., Fukushima, J., Warabi, T., & Barnes, G. R. (2013). Cognitive
915 processes involved in smooth pursuit eye movements: Behavioral evidence,

- 916 neural substrate and clinical correlation. *Frontiers in Systems Neuroscience*, 7.
917 <https://doi.org/10.3389/fnsys.2013.00004>
- 918 Fukushima, K., Yamanobe, T., Shinmei, Y., Fukushima, J., Kurkin, S., & Peterson, B.
919 W. (2002). Coding of smooth eye movements in three-dimensional space by
920 frontal cortex. *Nature*, 419(6903), 157–162.
- 921 Gagnon, D., Paus, T., Grosbras, M.-H., Pike, G. B., & O’Driscoll, G. A. (2006).
922 Transcranial magnetic stimulation of frontal oculomotor regions during
923 smooth pursuit. *Journal of Neuroscience*, 26(2), 458–466.
- 924 Gauthier, G. M., Vercher, J. L., Mussa Ivaldi, F., & Marchetti, E. (1988).
925 Oculo-manual tracking of visual targets: Control learning, coordination
926 control and coordination model. *Experimental Brain Research*, 73(1), 127–137.
927 <https://doi.org/10.1007/BF00279667>
- 928 Goldreich, D., Krauzlis, R. J., & Lisberger, S. G. (1992). Effect of changing feedback
929 delay on spontaneous oscillations in smooth pursuit eye movements of
930 monkeys. *Journal of Neurophysiology*, 67(3), 625–638.
931 <https://doi.org/10.1152/jn.1992.67.3.625>
- 932 Gottsdanker, R., Frick, J. W., & Lockard, R. B. (1961). IDENTIFYING THE
933 ACCELERATION OF VISUAL TARGETS. *British Journal of Psychology*, 52(1),
934 31–42. <https://doi.org/10.1111/j.2044-8295.1961.tb00765.x>
- 935 Grasse, K. L., & Lisberger, S. G. (1992). Analysis of a naturally occurring asymmetry
936 in vertical smooth pursuit eye movements in a monkey. *Journal of*
937 *Neurophysiology*, 67(1), 164–179. <https://doi.org/10.1152/jn.1992.67.1.164>
- 938 Heinen, S. J., Badler, J. B., & Ting, W. (2005). Timing and velocity randomization
939 similarly affect anticipatory pursuit. *Journal of Vision*, 5(6), 1–1.
940 <https://doi.org/10.1167/5.6.1>
- 941 Heinen, S. J., & Liu, M. (1997). Single-neuron activity in the dorsomedial frontal
942 cortex during smooth-pursuit eye movements to predictable target motion.
943 *Visual Neuroscience*, 14(5), 853–865.
944 <https://doi.org/10.1017/S0952523800011597>
- 945 Hlavac, M. (2022). *stargazer: Beautiful LATEX, HTML and ASCII tables from R*

946 *statistical output* [R].

947 Jarrett, C. B., & Barnes, G. (2002). Volitional scaling of anticipatory ocular pursuit
948 velocity using precues. *Cognitive Brain Research*, 14(3), 383–388.

949 [https://doi.org/10.1016/S0926-6410\(02\)00140-4](https://doi.org/10.1016/S0926-6410(02)00140-4)

950 Kao, G. W., & Morrow, M. J. (1994). The relationship of anticipatory smooth eye
951 movement to smooth pursuit initiation. *Vision Research*, 34(22), 3027–3036.

952 [https://doi.org/10.1016/0042-6989\(94\)90276-3](https://doi.org/10.1016/0042-6989(94)90276-3)

953 Ke, S. R., Lam, J., Pai, D. K., & Spering, M. (2013). Directional Asymmetries in
954 Human Smooth Pursuit Eye Movements. *Investigative Ophthalmology & Visual*

955 *Science*, 54(6), 4409. <https://doi.org/10.1167/iovs.12-11369>

956 Kowler, E., Martins, A. J., & Pavel, M. (1984). The effect of expectations on slow
957 oculomotor control—IV. Anticipatory smooth eye movements depend on

958 prior target motions. *Vision Research*, 24(3), 197–210.

959 Kowler, E., & McKee, S. P. (1987). Sensitivity of smooth eye movement to small
960 differences in target velocity. *Vision Research*, 27(6), 993–1015.

961 [https://doi.org/10.1016/0042-6989\(87\)90014-9](https://doi.org/10.1016/0042-6989(87)90014-9)

962 Kowler, E., Rubinstein, J. F., Santos, E. M., & Wang, J. (2019). Predictive Smooth
963 Pursuit Eye Movements. *Annual Review of Vision Science*, 5(1), 223–246.

964 <https://doi.org/10.1146/annurev-vision-091718-014901>

965 Kowler, E., & Steinman, R. M. (1979a). The effect of expectations on slow
966 oculomotor control—I. Periodic target steps. *Vision Research*, 19(6), 619–632.

967 [https://doi.org/10.1016/0042-6989\(79\)90238-4](https://doi.org/10.1016/0042-6989(79)90238-4)

968 Kowler, E., & Steinman, R. M. (1979b). The effect of expectations on slow
969 oculomotor control—II. Single target displacements. *Vision Research*, 19(6),

970 633–646. [https://doi.org/10.1016/0042-6989\(79\)90239-6](https://doi.org/10.1016/0042-6989(79)90239-6)

971 Krauzlis, R. J., & Lisberger, S. G. (1994). A model of visually-guided smooth pursuit
972 eye movements based on behavioral observations. *Journal of Computational*

973 *Neuroscience*, 1(4), 265–283.

974 Kreyenmeier, P., Kämmer, L., Fooker, J., & Spering, M. (2022). Humans Can Track
975 But Fail to Predict Accelerating Objects. *Eneuro*, 9(5),

- 976 ENEURO.0185-22.2022. <https://doi.org/10.1523/ENEURO.0185-22.2022>
- 977 Landelle, C., Montagnini, A., Madelain, L., & Danion, F. (2016). Eye tracking a
978 self-moved target with complex hand-target dynamics. *Journal of*
979 *Neurophysiology*, 116(4), 1859–1870. <https://doi.org/10.1152/jn.00007.2016>
- 980 Lenth, R. (2017). *Emmeans* [R]. <https://github.com/rvlenth/emmeans>
- 981 Lisberger, S. G., & Movshon, J. A. (1999). Visual motion analysis for pursuit eye
982 movements in area MT of macaque monkeys. *The Journal of Neuroscience: The*
983 *Official Journal of the Society for Neuroscience*, 19(6), 2224–2246.
984 <https://doi.org/10.1523/JNEUROSCI.19-06-02224.1999>
- 985 Lisberger, S., & Westbrook, L. (1985). Properties of visual inputs that initiate
986 horizontal smooth pursuit eye movements in monkeys. *The Journal of*
987 *Neuroscience*, 5(6), 1662–1673.
988 <https://doi.org/10.1523/JNEUROSCI.05-06-01662.1985>
- 989 MacAvoy, M. G., Gottlieb, J. P., & Bruce, C. J. (1991). Smooth-Pursuit Eye
990 Movement Representation in the Primate Frontal Eye Field. *Cerebral Cortex*,
991 1(1), 95–102. <https://doi.org/10.1093/cercor/1.1.95>
- 992 Makowski, D., Ben-Shachar, M., & Lüdecke, D. (2019). bayestestR: Describing
993 Effects and their Uncertainty, Existence and Significance within the Bayesian
994 Framework. *Journal of Open Source Software*, 4(40), 1541.
995 <https://doi.org/10.21105/joss.01541>
- 996 Maus, G. W., Potapchuk, E., Watamaniuk, S. N. J., & Heinen, S. J. (2015). Different
997 time scales of motion integration for anticipatory smooth pursuit and
998 perceptual adaptation. *Journal of Vision*, 15(2), 16–16.
999 <https://doi.org/10.1167/15.2.16>
- 1000 Montagnini, A., Souto, D., & Masson, G. (2010). Anticipatory eye-movements under
1001 uncertainty: A window onto the internal representation of a visuomotor prior.
1002 *Journal of Vision*, 10(7), 554–554. <https://doi.org/10.1167/10.7.554>
- 1003 Orban De Xivry, J.-J., & Lefèvre, P. (2007). Saccades and pursuit: Two outcomes of
1004 a single sensorimotor process: Saccades and smooth pursuit eye movements.
1005 *The Journal of Physiology*, 584(1), 11–23.

- 1006 <https://doi.org/10.1113/jphysiol.2007.139881>
- 1007 Pasturel, C., Montagnini, A., & Perrinet, L. U. (2018). ANEMO: Quantitative tools for
1008 the ANalysis of Eye MOVements. *Grenoble Workshop on Models and Analysis of*
1009 *Eye Movements, Grenoble, France.*
1010 <https://laurentperrinet.github.io/publication/pasturel-18-anemo>
- 1011 Pasturel, C., Montagnini, A., & Perrinet, L. U. (2020). Humans adapt their
1012 anticipatory eye movements to the volatility of visual motion properties.
1013 *PLOS Computational Biology*, 16(4), e1007438.
1014 <https://doi.org/10.1371/journal.pcbi.1007438>
- 1015 Price, N. S. C., Ono, S., Mustari, M. J., & Ibbotson, M. R. (2005). Comparing
1016 Acceleration and Speed Tuning in Macaque MT: Physiology and Modeling.
1017 *Journal of Neurophysiology*, 94(5), 3451–3464.
1018 <https://doi.org/10.1152/jn.00564.2005>
- 1019 Robinson, D. A. (1963). A Method of Measuring Eye Movement Using a Sieral
1020 Search Coil in a Magnetic Field. *IEEE Transactions on Bio-Medical Electronics*,
1021 10(4), 137–145. <https://doi.org/10.1109/TBMEL.1963.4322822>
- 1022 Rottach, K. G., Zivotofsky, A. Z., Das, V. E., Averbuch-Heller, L., Discenna, A. O.,
1023 Poonyathalang, A., & Leigh, R. J. (1996). Comparison of Horizontal, Vertical
1024 and Diagonal Smooth Pursuit Eye Movements in Normal Human Subjects.
1025 *Vision Research*, 36(14), 2189–2195.
1026 [https://doi.org/10.1016/0042-6989\(95\)00302-9](https://doi.org/10.1016/0042-6989(95)00302-9)
- 1027 Rubinstein, J. F., Singh, M., & Kowler, E. (2024). Bayesian approaches to smooth
1028 pursuit of random dot kinematograms: Effects of varying RDK noise and the
1029 predictability of RDK direction. *Journal of Neurophysiology*, 131(2), 394–416.
1030 <https://doi.org/10.1152/jn.00116.2023>
- 1031 Santos, E. M., & Kowler, E. (2017). Anticipatory smooth pursuit eye movements
1032 evoked by probabilistic cues. *Journal of Vision*, 17(13), 1–16.
1033 <https://doi.org/10.1167/17.13.13>
- 1034 Schlack, A., Krekelberg, B., & Albright, T. D. (2007). Recent History of Stimulus
1035 Speeds Affects the Speed Tuning of Neurons in Area MT. *The Journal of*

- 1036 *Neuroscience*, 27(41), 11009–11018.
1037 <https://doi.org/10.1523/JNEUROSCI.3165-07.2007>
- 1038 Schmerler, J. (1976). The Visual Perception of Accelerated Motion. *Perception*, 5(2),
1039 167–185. <https://doi.org/10.1068/p050167>
- 1040 Souto, D., & Kerzel, D. (2013). Like a rolling stone: Naturalistic visual kinematics
1041 facilitate tracking eye movements. *Journal of Vision*, 13(2), 9–9.
1042 <https://doi.org/10.1167/13.2.9>
- 1043 Souto, D., Montagnini, A., & Masson, G. S. (2008). Scaling of anticipatory smooth
1044 pursuit eye movements with target speed probability. *Journal of Vision*, 8(6),
1045 665–665. <https://doi.org/10.1167/8.6.665>
- 1046 Takeichi, N., Fukushima, J., Kurkin, S., Yamanobe, T., Shinmei, Y., & Fukushima, K.
1047 (2003). Directional asymmetry in smooth ocular tracking in the presence of
1048 visual background in young and adult primates. *Experimental Brain Research*,
1049 149(3), 380–390. <https://doi.org/10.1007/s00221-002-1367-3>
- 1050 Tychsen, L., & Lisberger, S. G. (1986). Visual motion processing for the initiation of
1051 smooth-pursuit eye movements in humans. *Journal of Neurophysiology*, 56(4),
1052 953–968. <https://doi.org/10.1152/jn.1986.56.4.953>
- 1053 Voeten, C. (2020). *buildmer: Stepwise elimination and term reordering for mixed-effects*
1054 *regression* [R].
- 1055 Watamaniuk, S. N. J., & Heinen, S. J. (2003). Perceptual and oculomotor evidence
1056 of limitations on processing accelerating motion. *Journal of Vision*, 3(11), 5.
1057 <https://doi.org/10.1167/3.11.5>
- 1058 Wu, X., Rothwell, A. C., Spering, M., & Montagnini, A. (2021). Expectations about
1059 motion direction affect perception and anticipatory smooth pursuit
1060 differently. *Journal of Neurophysiology*, 125(3), 977–991.
1061 <https://doi.org/10.1152/jn.00630.2020>
- 1062 Zago, M., Iosa, M., Maffei, V., & Lacquaniti, F. (2010). Extrapolation of vertical
1063 target motion through a brief visual occlusion. *Experimental Brain Research*,
1064 201(3), 365–384. <https://doi.org/10.1007/s00221-009-2041-9>

1065 **Supplementary material**

1066 **Final models for the LMM analysis**

1067 Exp 1A:

$$1068 aSPv \sim 1 + P(HS) + (1 + P(HS) \mid participant)$$

$$1069 aSPv \sim 1 + P(HS)*Tv_{N-1} + (1 + P(HS) + Tv_{N-1} \mid participant)$$

1070 Exp 1B, constant speed probability-mixtures:

$$1071 aSPv \sim 1 + P(v33) + axis + (1 + P(v33) + axis \mid participant)$$

$$1072 aSPv \sim 1 + P(v33)*Tv_{N-1} + (1 + P(v33) + Tv_{N-1} \mid participant)$$

1073 Exp 2A-B, accelerating target probability-mixtures:

$$1074 aSPv \sim 1 + prob + axis + exp + axis:exp + (1 + prob + axis \mid participant)$$

1075 Exp 3, comparison between fully predictable blocks:

$$1076 aSPv \sim 1 + v0*accel + (1 + v0 \mid participant)$$

1077 Exp3, categorical model for pairwise comparisons:

$$1078 aSpv \sim 1 + condition + (1 \mid participant)$$

1079

1080

1081 LMM analysis - result tables

1082

Exp1A: Anticipatory Parameters

	<i>Dependent variable:</i>
	aSPv
P(HS)	3.488 ^{***} (3.138, 3.838) t = 19.541 p = 0.000
Constant	2.759 ^{***} (2.036, 3.482) t = 7.480 p = 0.000
<hr/> Random Effects	
Groups	3
sd(Constant)	0.77
sd(P(HS))	0.33
<hr/>	
<i>Note:</i>	* p < 0.01; ** p < 0.001; *** p < 1e-04

1083

1084

Exp 1A: Anticipatory Parameters– Sequential Effects

	<i>Dependent variable:</i>	
	aSPv	
Tv _{N-1} [LS]	-0.501 ^{***}	(-0.663, -0.340)
	t = -6.073	
	p = 0.000	
P(HS)	4.357 ^{***}	(3.983, 4.732)
	t = 22.827	
	p = 0.000	
P(HS):Tv _{N-1} [LS]	-2.744 ^{***}	(-3.102, -2.386)
	t = -15.030	
	p = 0.000	
Constant	4.427 ^{***}	(3.801, 5.053)
	t = 13.853	
	p = 0.000	
<hr/>		
Random Effects		
Groups	3	
sd(Constant)	0.70	
sd(P(HS))	0.10	
sd(Tv _{N-1} [LS])	0.29	

Note: * p < 0.01; ** p < 0.001; *** p < 1e-04

1085

1086

1087

Exp 1B: Anticipatory Parameters – Const Speed

<i>Dependent variable:</i>	
aSPv	
P(v33)	2.743 ^{***} (1.824, 3.663) t = 5.847 p = 0.000
Axis[vert.]	-0.740 (-1.464, -0.016) t = -2.002 p = 0.046
P(v33):Axis[vert.]	-0.674 ^{***} (-0.985, -0.363) t = -4.252 p = 0.00003
Constant	2.707 ^{***} (1.740, 3.673) t = 5.490 p = 0.00000
Random Effects	
Groups	13
sd(Constant)	1.82
sd(P(v33))	1.68
sd(Axis[vert.])	1.32

Note: * p < 0.01; ** p < 0.001; *** p < 1e-04

1088

1089

1090

Exp 1B: Anticipatory Parameters – Const Speed - Sequential Effects

<i>Dependent variable:</i>	
aSPv	
Tv _{N-1} [v11]	-0.613 ^{***} (-0.882, -0.345) t = -4.482 p = 0.00001
P(v33)	1.380 [*] (0.437, 2.323) t = 2.869 p = 0.005
Tv _{N-1} [v11]:P(v33)	0.823 ^{**} (0.383, 1.263) t = 3.663 p = 0.0003
Constant	3.948 ^{***} (3.114, 4.781) t = 9.279 p = 0.000
Random Effects	
Groups	13
sd(Constant)	1.58
sd(P(v33))	1.67
sd(Tv _{N-1} [v11])	0.43

Note: * p < 0.01; ** p < 0.001; *** p < 1e-04

1091

1092

1093

1094

1095

Exp 2A-B: Anticipatory Parameters – Accelerating Target

	<i>Dependent variable:</i>
	aSPv
P(vdec)	1.884 ^{***} (1.111, 2.657) t = 4.779 p = 0.00001
Axis[vert.]	-0.460 (-1.264, 0.343) t = -1.123 p = 0.262
Exp.[const.Time]	1.683 ^{***} (1.410, 1.956) t = 12.086 p = 0.000
Exp.[const.Time]:Axis[vert.]	-1.651 ^{***} (-2.027, -1.275) t = -8.611 p = 0.000
Constant	3.041 ^{***} (2.099, 3.983) t = 6.326 p = 0.000
<hr/>	
Random Effects	
Groups	16
sd(Constant)	1.96
sd(P(V3))	1.58
sd(Axis[vert.])	1.66
<hr/>	
Note:	* p < 0.01; ** p < 0.001; *** p < 1e-04

1096

1097

Exp 3: Anticipatory Parameters – Parametric Variables

<i>Dependent variable:</i>	
aSPv	
V0	0.246 ^{***} (0.149, 0.343) t = 4.963 p = 0.00000
Accel	0.017 [*] (0.004, 0.030) t = 2.640 p = 0.009
V0:Accel	0.001 [*] (0.0004, 0.002) t = 2.905 p = 0.004
Constant	0.364 (-0.324, 1.052) t = 1.037 p = 0.300
Random Effects	
Groups	7
sd(Constant)	0.95
sd(v0)	0.14
Groups	7

Note: * p < 0.01; ** p < 0.001; *** p < 1e-04

1098

1099 **Exp 3: Pairwise comparisons**

1100

1101

1102	contrast	estimate	SE	df	t.ratio	p.value
1103	V1a - V1c	0.640	0.140	8749	4.559	<.0001
1104	V1a - V1d	0.934	0.143	8749	6.545	<.0001
1105	V1a - V2a	-2.236	0.136	8749	-16.396	<.0001
1106	V1a - V2c	-1.037	0.140	8749	-7.430	<.0001
1107	V1a - V2d	-1.503	0.139	8749	-10.779	<.0001
1108	V1a - V3a	-4.114	0.130	8749	-31.598	<.0001
1109	V1a - V3c	-3.320	0.135	8749	-24.626	<.0001
1110	V1a - V3d	-2.679	0.136	8749	-19.647	<.0001
1111	V1c - V1d	0.294	0.142	8749	2.065	0.0390
1112	V1c - V2a	-2.876	0.136	8749	-21.149	<.0001
1113	V1c - V2c	-1.677	0.139	8749	-12.051	<.0001
1114	V1c - V2d	-2.143	0.139	8749	-15.417	<.0001
1115	V1c - V3a	-4.754	0.130	8749	-36.624	<.0001
1116	V1c - V3c	-3.960	0.134	8749	-29.472	<.0001
1117	V1c - V3d	-3.319	0.136	8749	-24.415	<.0001
1118	V1d - V2a	-3.170	0.138	8749	-22.921	<.0001
1119	V1d - V2c	-1.971	0.141	8749	-13.932	<.0001
1120	V1d - V2d	-2.437	0.141	8749	-17.251	<.0001
1121	V1d - V3a	-5.048	0.132	8749	-38.177	<.0001
1122	V1d - V3c	-4.254	0.137	8749	-31.095	<.0001

*n.s.

1123	V1d - V3d	-3.613	0.138	8749	-26.115	<.0001	
1124	V2a - V2c	1.199	0.135	8749	8.875	<.0001	
1125	V2a - V2d	0.733	0.135	8749	5.434	<.0001	
1126	V2a - V3a	-1.878	0.125	8749	-14.982	<.0001	
1127	V2a - V3c	-1.084	0.130	8749	-8.326	<.0001	
1128	V2a - V3d	-0.443	0.132	8749	-3.362	0.0008	
1129	V2c - V2d	-0.466	0.138	8749	-3.372	0.0008	*effect in the
1130							opposite direction
1131	V2c - V3a	-3.077	0.129	8749	-23.872	<.0001	
1132	V2c - V3c	-2.283	0.134	8749	-17.100	<.0001	
1133	V2c - V3d	-1.642	0.135	8749	-12.153	<.0001	
1134	V2d - V3a	-2.611	0.129	8749	-20.288	<.0001	
1135	V2d - V3c	-1.818	0.133	8749	-13.631	<.0001	
1136	V2d - V3d	-1.176	0.135	8749	-8.719	<.0001	
1137	V3a - V3c	0.794	0.124	8749	6.413	<.0001	
1138	V3a - V3d	1.435	0.125	8749	11.442	<.0001	
1139	V3c - V3d	0.641	0.130	8749	4.927	<.0001	
1140							
1141	Degrees-of-freedom method: containment						
1142	P value adjustment: BH method for 36 tests						

